ACKNOWLEDGMENT

The author is grateful to his director, Professor William Kozicki, not only for his guidance and encouragement throughout the course of this research, but also for his excellent ideas. He wishes to thank also the faculty and his fellow students for their suggestions, particularly Mr. C. Tiu for reviewing the manuscript, and Mr. T.R. Lion for translating a Japanese paper. He also wishes to acknowledge the National Research Council for the financial assistance received under the grant No. A-1602.

C. H. Chou

TABLE OF CONTENTS

TABLE OF CONTENTS (Continued)

LIST OF FIGURES

LIST OF FIGURES (Continued)

I - ABSTRACT

Two general equations for predicting the flow rate-pressure drop relationships and maximum velocity for the steady, isothermal, laminar flow of an incompressible, time-independent non-Newtonian fluid in straight ducts of arbitrary uniform cross section are proposed.

The equations are expressed in terms of two constants which characterize the geometry of the flow cross section, and a function of shear stress which represents the shear rate, used to characterize the behavior of the fluid model. Numerical values of the geometric parameters have been determined and are given for circular tubes, parallel plates, concentric annuli, rectangular ducts, elliptic ducts and isosceles triangular ducts. Comparisons made with available experimental data and prior analyses for Newtonian, power law, Bingham, and Rabinowitsch fluids are found to be in good agreement.

II - INTRODUCTION

A knowledge of the flow rate-pressure drop relationships for Newtonian and non-Newtonian flow in any shape of conduit is of importance in connection with the transportion of fluids, flow equipment design, flow of molten plastics in extrusion apparatus and flow of drilling muds in annular spaces.

Although the equation of motion together with an empirical fluid model often enables one to obtain the required relationship, accurate solutions for some complicated geometries require elaborate numerical efforts. For example, Sparrow (7) solved the case of laminar flow of Newtonian fluid in isosceles triangular ducts.

By way of extrapolation from the Rabinowitsch-Mooney equation (8), Kozicki (32) postulated that two constants may be used to characterise the flow through any arbitrary cross section. Consequently, with a given fluid and the applicable geometrical parameters, the generalised Rabinowitsch and Mooney equation can be readily integrated to obtain the generalised flow rate-pressure drop relationship. By an analogous approach, the maximum velocity has also been generalised in the present work.

Certain effects which may cause the flow system to deviate from the assumed model will be discussed in Chapter IV.

III - LITERATURE SURVEY

For the flow of Newtonian fluids in circular tubes, the famous Hagen-Poiseuille law (1, 2, 3) was derived in 1839. Buckingham and Reiner (4, 5) first obtained the volumetric flow rate expression for Bingham flow. For pseudoplastic fluids, a corresponding expression can be derived easily by a procedure similar to that followed for the former fluids (6).

In the case of flow between parallel plates, the derivations are straightforward (1, 8, 9).

The solution to the Newtonian flow through annuli problem has been obtained (1, 8). Fredrickson and Bird (9) have used analytical and numerical techniques to solve the corresponding problem for Bingham plastic and pseudoplastic fluids. Reiner (10) adopted the same method to arrive at a similar solution for a Rabinowitsch fluid, as a special case of the "general" fluid (10).

Cornish (11) and Lee and Tedrow (12) derived separably a theoretical equation for laminar Newtonian flow in rectangular ducts. Allen (13), Davis (14) and Schiller (15) have presented some experimental data. Analytical expressions may also be found in another source (16). An illustration of the agreement

obtained in a comparison with experimental data is available (17). Schecter (18) applied the variational principle to solve the problem of pseudoplastic flow in rectangular ducts. Wheeler and Wissler (19) employed the over-relaxation method to solve the same problem and substantiated their result with experimental measurements.

Analytical solutions for Newtonian flow through elliptic ducts have been derived (16, 17). Mizushina, Mitsuishi and Nakamura (20) obtained a solution for the flow of power law fluids by application of the variational principle. Solution for other fluids have not been presented to date.

Sparrow (39) has obtained a solution to the problem of laminar flow in isosceles triangular ducts applicable to Newtonian fluids. Before this, exact solutions were available for the equilateral and the right-isosceles triangles (17, 22), two special cases of Sparrow's solution.

Several recent papers have investigated the laminar-turbulent transition problem. Ryan and Johnson (23) proposed a general stability parameter Z for pipe flow and demonstrated the utility of Z in predicting the transition from laminar to turbulent flow in the isothermal flow of power law fluids. Hanks and Christiansen (24) extended the range of applicability of Z to include non-isothermal flow of pseudoplastic fluids, showing the

temperature invariance of Z. Since Z is geometry dependent, Hanks (25) proposed another stability factor K, independent of geometry. Critical Reynolds numbers for Newtonian flow in pipes, concentric annuli and parallel plates have been calculated and compared with experimental data (25). In the case of non-Newtonian fluids, only the pseudoplastic case has been theoretically investigated (24). Further study appears to be needed in this area.

IV - NON-NEWTONIAN BEHAVIOR

A. Definitions

Deformation is a movement of parts or particles of a material body, relative to one another, such that the continuity of the body is not destroyed. A fluid is a substance that deforms continuously only when subjected to a shear stress, no matter how small the shear stress may be. The material is said to flow if, under the action of finite forces, the deformation of the body increases with time continuously and indefinitely. A material may be caused to flow, i.e., becomes fluid, by varying temperature and force field. Fluidity is the term used to describe the temporary state of matter.

B. Basic Material Properties

Idealized materials represent a necessary starting point in consideration of the flow of fluids, since the behavior of actual fluids is usually defined and best visualized in terms of deviations from these ideals. Polymeric melts and solutions display some of the properties commonly associated with both solid and liquid states (7).

An ideal or elastic solid is defined by Hooke's law:

$$T_T = E \frac{L - L_0}{L_0} = E \gamma_T \qquad (4-1)$$

The constant of proportionality E, referred to as Young's modulus, may be considered to be a physical property of the material. When the solid is subjected to a shearing stress, the equation used to describe this situation is

$$T = G \frac{\Delta L}{L_o} = G \gamma_e \qquad (4\text{-}2)$$

The chief characteristics of an elastic solid are (a) the direct proportionality between stress and strain, and (b) the instantaneous change in shape of the object when the stress is changed. An ideal coil spring may be considered to be a mechanical model having the same behavior as an elastic solid (7).

An ideal or Newtonian liquid is similarly defined by Newton's law of viscosity:

$$T_{yx} = \mu_F \frac{du}{dy} = \mu_F \frac{d\gamma_e}{dt} \qquad (4\text{-}3)$$

It is thus seen that under a given shearing force, the total strain in a solid is constant; whereas the rate of strain is constant in a Newtonian fluid. The mathematical approach to non-Newtonian behavior assumes that materials exist which have the characteristics of both the Newtonian fluid and elastic solid. Mechanical models may enable one to visualize the actual flow behavior.

Newtonian behavior has been found to be common to the following systems: (a) all gases and (b) all liquids or solutions of low molecular weight materials (29).

In gases, the Brownian motion of small molecules causes those in faster moving laminae occasionally to move laterally into regions of lower velocity where they lose their excess velocity by collision with the slower-moving molecules. In a liquid, momentum is interchanged not by direct collision of the molecules, but rather by means of a mechanism in which the faster moving molecule drags the slower one along owing to the attractive forces between them. The molecules, in many cases, will be separated again before this momentum interchange is complete (30).

Non-Newtonian behavior is commonly observed in the following types of systems: (a) Solutions or melts of high-molecular-weight polymeric materials, except when unusually dilute. (b) Suspensions of solids in liquids (29).

Time-independent non-Newtonian behavior of polymeric melts and solutions is attributed to the following two characteristics (7) of molecular structure: (a) The asymmetric shape of the molecules results in an orientation of the particles when a velocity

gradient is imposed on the polymer molecules (26, 29). This orientation causes the molecules to become progressively more perfectly aligned as the velocity gradient of the fluid is increased. At extremely low shear rates, the random molecular (Brownian) motion disrupts the alignment, and the material behaves as a Newtonian fluid. Conversely, at extremely high shear rates, the disrupting effects of Brownian motion are negligible. However, further changes in shear rate in this region do not affect appreciably the degree of orientation, and as a consequence, the material again approaches Newtonian behavior. In the intermediate shear rate region, both effects, viz., Brownian motion and alignment associated with velocity gradient are important. A mechanism of momentum interchange occurring in the intermediate shear rate region is more efficient than that in the very low shear rate and also very high shear rate regions. For the excess energy transferred to the end of the molecule in high-velocity region is simply transmitted to the other end of the same molecule, where it is lost by direct collision. Therefore, a complete flow curve, a relation between the shear stress and shear rate, consists of three regions - a Newtonian region at both low and high rates of shear, and a pseudoplastic region at medium rate of shear. In general, the viscosity of non-Newtonian fluids is higher than that of Newtonian fluids at the same

shear rate. (b) The size of the flowing elements (if they are groups of molecules rather than single molecules) would be decreased progressively by increasing the shear stress. The restoring tendencies are due to intermolecular forces; the effects of shear rate and temperature on the size of the flowing elements are similar to those on alignment discussed above. Hence, three regions of a flow curve can again be observed.

Numerous empirical equations, or "models", have been proposed to express the time-independent relation between shear stress and shear rate. This time-independent rheological behavior of most fluids can be expressed by a generalized form (1):

$$\tau_{yx} = -\eta \frac{du_x}{dy} \qquad (4-6)$$

Six models are given in Appendix I.

A number of additional types of non-Newtonian behavior are possible. For example, fluids that show a limited decrease in apparent viscosity with time under a suddenly applied constant stress τ_{yx} are called thixotropic, whereas those that show an increase in η with time are called rheopectic (1). One procedure of analysis is so-called loop technique in which a substance is subjected to an increase in shear rate and then to a decrease in shear rate, returning to a shear of zero. If no time dependence exists, the two curves should be coincident. Fluids that partially return to their original

form when the applied stress is released are called visco-elastic.

C. Some Important Effects

1. Effect of Pressure on Flow Properties

Since the viscosity of a liquid depends on the magnitude of the intermolecular forces and the intermolecular distances, compression of a liquid should result in large increase in viscosity (7). For many liquids, this effect is not great. However, the possible effect is enormous: The viscosity of isobutanol at 12,000 atm. is 790 times that of atmospheric value at the same temperature (7, 42).

2. Effect of Temperature on Flow Properties

An increase in the temperature of the fluid will suppress the non-Newtonian tendency because of Brownian motion. For instance, the flow behavior index n of polyethylene at a shear rate of 100 sec^{-1} is 0.32 at 108°C and 0.49 at 230°C (7).

For Newtonian fluids, the effect of temperature on viscosity may be expressed by the usual exponential equation:

$$\mu_T \ (= \eta) = A e^{\frac{E}{RT}} \qquad (4\text{-}5)$$

For non-Newtonian fluids, the activation energy varies with both temperature and shear rate. The above equation is limited

to temperature regions in which the flow behavior index remains reasonably constant. The activation energy E for polyethylene at a shear rate of 100 sec^{-1} is 7 kcal/gm-mole at 200°C (7).

3. End Effects

The case of pipe flow will be discussed. An entrance length for laminar Newtonian flow on the order of $L_e = 0.03 N_{Re} D$ is required for build-up to the parabolic profiles. Collins and Schowalter (46) solved the entrance region problem for pseudo-plastics and reported the numerical values of $2L_e / Re' D$.

The pressure loss between the entrance of the pipe $x = 0$ and some point x_1 in the fully developed region may be expressed as

$$\frac{|\Delta p|}{\frac{1}{2} \rho U^2} = \frac{2^{n+2} \left(\frac{1+3n}{n}\right)^n}{N_{Re'}} \left(\frac{x_1}{R}\right) + C \qquad (4\text{-}6)$$

Values of C have been calculated (46).

A method of applying a correction for the entrance effect to the pressure gradient is outlined below (33).

$$\tau_0 = \frac{D}{4} \left(\frac{|\Delta p|}{L + ND}\right) = \beta \left(\frac{8U}{D}\right) \qquad (4\text{-}7)$$

$$N = \frac{|\Delta p|}{4\beta} \cdot \frac{L}{D} \qquad (4\text{-}8)$$

Here, ND represents a fictitious tube length which when added to the actual length enables one to calculate the pressure gradient in the steady flow section.

For high Reynolds numbers, uncorrected pressure gradients may lead to large errors. For example, one case in Bagley's data (41) showed a 30% deviation (42).

Gaskins and Philippoff (34) have presented an analysis for problem of contraction, in the flow of a pseudoplastic fluid, associated with the rearrangement of the velocity profile in the exit region. They assumed that there is conservation of momentum associated with the bulk motion of the fluid between the discharge end of the tube and the section downstream at which the velocity rearrangement is complete. An analogous solution was obtained by Yen and Tien (35) for a Bingham plastic fluid. Kosicki and Yuan (36) applied the principle of conservation of energy to the same problems and obtained different solutions. The results were expressed in terms of the discharge coefficient U/U_g. The values obtained by Kosicki and Yuan are smaller than those determined by the other authors.

McIntosh (38, 42) performed an analysis to account for the swelling of viscoelastic fluids in the exit region. When a recoverable elastic shear strain is imparted to a fluid, a swelling will occur in the exit region.

4. Elasticity

It has been suggested that limitations encountered with inelastic fluids are of no consequence in situations in which the fluid is sheared continuously and extensively in a single direction, as elastic effects would be manifested primarily as "end effects" in the regions where the shear begins and ends (7). Several authors (21, 37) have shown that the above view is justified in the case of flow through a pipe of constant cross section.

5. Kinetic Energy Correction Factor

The term $U^2/2g_c$ in the Bernoulli equation is modified in order to take the velocity distribution into account. This can be done by defining a kinetic-energy correction factor (7, 29).

$$E_k = \frac{U^2}{\alpha g_c} = \frac{1}{UR^2} \int_0^R \frac{u^3 r\,dr}{g_c} \qquad (4\text{-}9)$$

Dodge (29) has integrated the above equation and obtained an expression for the flow of a pseudoplastic fluid in the fully developed laminar flow region.

$$\alpha = \frac{(4n+2)(5n+3)}{3(3n+1)^2} \qquad (4\text{-}10)$$

6. Viscous Dissipation

In an infinitesimal volume element of fluid, situated in the space between two parallel plates through which the fluid is supposed flowing, energy is dissipated at a rate p which is equal to the product of the force and the velocity. On the basis of unit volume,

$$p = \frac{(T\,dx\,dz)\,du}{dx\,dy\,dz} = T\frac{du}{dy} \tag{4-11}$$

For pseudoplastic fluid,

$$p = K\left(\frac{du}{dy}\right)^{1+n} \tag{4-12}$$

7. Slip Velocity

The case of pipe flow will be discussed. The velocity distribution without slip velocity at the wall is

$$u = \frac{R}{T_w}\int_{\frac{R}{T_w}T}^{T_w} f(T)\,dT \tag{4-13}$$

where $f(T) = -du/dr$.

The velocity distribution with an effective slip s at the pipe wall is

(i.e., $u = s\,(T_w)$ at $r = R$)

$$u = s\,(T_w) + \frac{R}{T_w}\int_{\frac{R}{T_w}T}^{T_w} f(T)\,dT \tag{4-14}$$

Then,

$$Q = \int_0^R 2\pi r u \, dr$$

$$= \pi R^2 S + \frac{\pi R}{T_w} \int_0^{T_w} f(T) \left(\frac{T}{T_w} R\right)^2 dT \qquad (4\text{-}15)$$

$$\frac{4Q}{\pi R^3 T_w} = \frac{4S}{R T_w} + \frac{4}{T_w^4} \int_0^{T_w} T^2 f(T) \, dT \qquad (4\text{-}16)$$

If

$$\zeta(T_w) = \frac{S}{T_w} \qquad (4\text{-}17)$$

$$\phi(T_w) = \frac{4}{T_w^4} \int_0^{T_w} T^2 f(T) \, dT \qquad (4\text{-}18)$$

$$1/\eta' = \pi R^3 T_w / 4\phi \qquad (4\text{-}19)$$

Eq. (4-16) becomes

$$\frac{1}{\eta'} = \frac{4}{R} \zeta(T_w) + \phi(T_w) \qquad (4\text{-}20)$$

Several authors (47, 48, 49, 50) have discussed this problem and pointed out that in the absence of a slip velocity, the curves of $\frac{1}{\eta'}$ vs. T_w for different pipe diameters should coincide and give a direct plot of

$$\frac{1}{\eta'} = \phi(T_w) \qquad (4\text{-}21)$$

generalized Rabinowitsch-Mooney equation.

The Rabinowitsch-Mooney equation for pipes may be expressed in the form

$$-\frac{du}{dn} = \frac{1}{4} T_w \frac{d\left(\frac{2U}{r_H}\right)}{d T_w} + \frac{3}{4}\left(\frac{2U}{r_H}\right) \qquad (5\text{-}1)$$

and for parallel plates, the similar expression is

$$-\frac{du}{dn} = \frac{1}{2} T_w \frac{d\left(\frac{2U}{r_H}\right)}{d T_w} + \left(\frac{2U}{r_H}\right) \qquad (5\text{-}2)$$

In order to generalize the Rabinowitsch-Mooney equation, it is first assumed that the average values of $-du/dn$ and T_w for any arbitrary cross section evaluated along the circumference might be used. Thus, the equation assumes the following form:

$$\frac{1}{C}\oint_c f(T_w)\, dl = a T_o \frac{d\left(\frac{2U}{r_H}\right)}{d T_o} + b\left(\frac{2U}{r_H}\right) \qquad (5\text{-}3)$$

where c = duct circumference

a, b = geometric parameters

$$T_o = \frac{1}{C}\oint_c T_w\, dl = r_H\left(-\frac{dp'}{dx}\right) \qquad (5\text{-}4)$$

$$f(T_w) = -\frac{du}{dn} \qquad (5\text{-}5)$$

It is further assumed that the left-hand side of Equation (5-3) might be approximated by $f(T_o)$, since this is true for both Newtonian and Bingham fluids (32) as well as for flow through pipes and parallel plates. Thus, the final form of the generalised Rabinowitsch-Mooney equation obtained and which will be used here is

$$f(T_o) = a\,T_o\,\frac{d\left(\frac{2U}{r_H}\right)}{d\,T_o} + b\left(\frac{2U}{r_H}\right) \qquad (5\text{-}6)$$

Kozicki (Appendix V) has also proposed a more general Rabinowitsch-Mooney equation including the effective slip velocity. Integration of Eq. (5-6) results in

$$\frac{2U}{r_H} = \frac{T_o^{-\frac{b}{a}}}{a}\int_{T_y}^{T_o} T^{\frac{b}{a}-1} f(T)\,dT \qquad (5\text{-}7)$$

Postulate 2:

In order to obtain the numerical values of "a" and "b" from Newtonian flow data alone, it is necessary to seek another relation which can be solved simultaneously with Eq. (5-7). By a similar argument, one may generalise the equation for maximum velocity as follows.

The maximum velocity for pipes is

$$u_{max} = \frac{R}{T_w} \int_{T_y}^{T_w} f(T)\, dT = \frac{2\tau_H}{T_w} \int_{T_y}^{T_w} f(T)\, dT \qquad (5\text{-}8)$$

and for parallel plates, it is

$$u_{max} = \frac{y_o}{T_w} \int_{T_y}^{T_w} f(T)\, dT = \frac{\tau_H}{T_w} \int_{T_y}^{T_w} f(T)\, dT \qquad (5\text{-}9)$$

The equation, which is the Postulate 2,

$$\frac{2U_{max}}{\tau_H} = \frac{1}{a T_o} \int_{T_y}^{T_o} f(T)\, dT \qquad (5\text{-}10)$$

satisfies the two above special cases.

The ratio u_{max}/U is thus given by

$$\frac{U_{max}}{U} = \frac{\int_{T_y}^{T_o} f(T)\, dT}{T_o^{-\frac{b}{a}} \int_{T_y}^{T_o} T^{\frac{b}{a}-1} f(T)\, dT} \qquad (5\text{-}11)$$

Concerning the validity of these postulates, it should be pointed out that the postulates 1 and 2 are rigorous for any fluid flowing through pipes and between parallel plates. Two of the most common non-Newtonian fluids, viz., power law and Bingham fluids, will be examined here. Postulate 1 will be considered first:

(a) Power law fluids:

$$f(\tau_w) = -\frac{du}{dn} = \left(\frac{\tau_w}{K}\right)^{\frac{1}{n}} \tag{5-12}$$

and

$$\tau_o = \left(-r_H \frac{dP'}{dx}\right) = K \left(\frac{2U}{r_H} \frac{a+bn}{n}\right)^n \tag{5-13}$$

(1) For pipes, $a = 1/4$, $b = 3/4$, and we obtain

$$\tau_o = \tau_w = K \left(\frac{2U}{r_H} \frac{1+3n}{4n}\right)^n \tag{5-14}$$

(2) For parallel plates, $a = 1/2$, $b = 1$, and we find

$$\tau_o = \tau_w = K \left(\frac{2U}{r_H} \frac{1+2n}{2n}\right)^n \tag{5-15}$$

(b) Bingham plastic fluids:

$$f(\tau) = \frac{\tau - \tau_y}{\beta} \tag{5-16}$$

and

$$\tau_o = \left(-r_H \frac{dP'}{dx}\right) = \frac{2U\beta}{r_H} \left[\frac{1}{a+b} - \frac{1}{b} \left(\frac{\tau_y}{\tau_o}\right) + \frac{a}{(a+b)b} \left(\frac{\tau_y}{\tau_o}\right)^{\frac{b}{a}+1} \right]^{-1} \tag{5-17}$$

(1) For pipes,

$$\tau_w = (-r_H \frac{dP'}{dx}) = \frac{2U\beta}{r_H} \left[1 - \frac{4}{3} \frac{\tau_y}{\tau_w} + \frac{1}{3} \left(\frac{\tau_y}{\tau_w}\right)^4 \right]^{-1} \qquad (5\text{-}18)$$

(2) For parallel plates,

$$\tau_w = (-r_H \frac{dP'}{dx}) = \frac{2U\beta}{r_H} \left[\frac{2}{3} - \frac{\tau_y}{\tau_w} + \frac{1}{3} \left(\frac{\tau_y}{\tau_w}\right)^3 \right]^{-1} \qquad (5\text{-}19)$$

Equation (5-14) reduces to the familiar Hagen-Poiseuille law, flow equation for Newtonian fluids in pipes, when n = 1. Equation (5-15) is also an exact solution (Ref. 7, pp. 55). Equation (5-18) is known as the Buckingham-Reiner Equation (Ref. 1, pp. 58). The equation for Bingham flow through parallel plates, i.e., Equation (5-19), is also identical with the rigorous solution (Ref. 9, Equation 20), as expected.

Postulate 2 is examined in the following,

(a) For power law fluids, Eq. (5-10) yields

$$\frac{2\,u_{max}}{r_H} = \frac{n}{n(1+n)} \left(\frac{\tau_0}{K}\right)^{\frac{1}{n}} \qquad (5\text{-}20)$$

(b) For parallel plates, Eq. (5-20) reduces to

$$\frac{2\,u_{max}}{r_H} = \frac{4n}{1+n} \left(\frac{\tau_w}{K}\right)^{\frac{1}{n}} \qquad (5\text{-}21)$$

(2) For parallel plates, Eq. (5-20) reduces to

$$\frac{2u_{max}}{r_H} = \frac{2n}{1+n}\left(\frac{\tau_w}{K}\right)^{\frac{1}{n}} \qquad (5\text{-}22)$$

(b) For Bingham plastic fluids, Eq. (5-10) yields

$$\frac{2u_{max}}{r_H} = \frac{\tau_o}{2a\beta}\left[1+\left(\frac{\tau_y}{\tau_o}\right)^2 - 2\left(\frac{\tau_y}{\tau_o}\right)\right] \qquad (5\text{-}23)$$

(1) For pipes, Eq. (5-23) reduces to

$$\frac{2u_{max}}{r_H} = \frac{2\tau_w}{\beta}\left[1+\left(\frac{\tau_y}{\tau_w}\right)^2 - 2\left(\frac{\tau_y}{\tau_w}\right)\right] \qquad (5\text{-}24)$$

(2) For parallel plates, Eq. (5-23) becomes

$$\frac{2u_{max}}{r_H} = \frac{\tau_w}{\beta}\left[1+\left(\frac{\tau_y}{\tau_w}\right)^2 - 2\left(\frac{\tau_y}{\tau_w}\right)\right] \qquad (5\text{-}25)$$

Equations (5-21, 22, 24) are identical with standard solutions (Ref. 6, Eq. 9-22; Ref. 7, Eq. 51; and Ref. 8, Eq. 9-15 respectively). Equation (5-25) is shown in Appendix IV.

For concentric annuli, it is convenient to define the parameter k, the ratio of inner to outer radius of the annuli. Then parallel plates and pipes are two limiting cases of annuli, i.e., $k = 1$ and $k = 0$ respectively. Since it has been postulated that a and b are geometric constants only, it follows that a and b are functions of k only. In principle, two measurements, i.e., an average velocity and a maximum velocity, at a given pressure drop for any fluid flowing through a

specific annulus will enable us to obtain a and b by solving Eq. (5-7) and Eq. (5-10) simultaneously. However, the Newtonian data will be chosen. The reasons for doing this will be discussed in Chapter VI. Values of a and b for ducts of different shaped cross sections will also be determined in the next chapter.

VI - THE GEOMETRIC CONSTANTS

The appropriate values of the two geometrical constants a and b were determined for ducts of various shapes of cross section. Since Newtonian data were more complete and accurate than corresponding data for other fluid models, a and b were determined using Newtonian flow data. Furthermore, non-Newtonian fluids may be considered as fluids whose behavior deviates from the Newtonian fluids.

The following values of a and b applicable to pipes and parallel plates are readily deduced by examination of the Rabinowitsch-Mooney equation applicable to these flow cross sections.

A. Pipes.

$a = 1/4, \quad b = 3/4$

B. Parallel plates.

$a = 1/2, \quad b = 1$

It should be emphasized that the values of a and b for pipes and parallel plates are rigorous for any fluid, since they appear, as stated above, in the original Rabinowitsch-Mooney equation.

C. Annuli - Utilizing the analytical solutions for the bulk velocity and maximum velocity determined for Newtonian fluids, the values of a and b can be expressed uniquely as functions of k:

$$a + b = \frac{(1 - k)^2}{1 + k^2 - \frac{1 - k^2}{\ln \frac{1}{k}}} \qquad (6\text{-}1)$$

$$a = \frac{(1 - k)^2}{4\left\{1 - \frac{1 - k^2}{2 \ln \frac{1}{k}}\left[1 - \ln\left(\frac{1 - k^2}{2 \ln \frac{1}{k}}\right)\right]\right\}} \qquad (6\text{-}2)$$

where k is the ratio of inner to outer radius of the annulus.

Substitution of Eq. (6-2) into Eq. (6-1) yields the value of b.

D. Rectangular ducts - Similarly, for rectangular ducts, it is found that

$$a + b = \frac{3}{2(1 + E)^2\left[1 - \frac{192}{\pi^5} E\left(\tanh \frac{\pi}{2E} + \frac{1}{3^5} \tanh \frac{3\pi}{2E} + \ldots\right)\right]} \qquad (6\text{-}3)$$

and

$$a = \left\{2(1 + E)^2\left[1 + 4\left(\frac{-1}{\left(\frac{\pi}{2}\right)^3 \cosh \frac{\pi}{2E}} + \frac{1}{\left(\frac{3\pi}{2}\right)^3 \cosh \frac{3\pi}{2E}} + \frac{-1}{\left(\frac{5\pi}{2}\right)^3 \cosh \frac{5\pi}{2E}}\right)\right]\right\}^{-1} \qquad (6\text{-}4)$$

where

$$E = b'/a' = \frac{\text{half length of minor side}}{\text{half length of major side}}$$

E. Elliptic ducts - The geometric constants are given by

$$a + b = \frac{\pi^2}{8 E_o^2} \left[\left(\frac{b'}{a'}\right)^2 + 1 \right] \qquad (6\text{-}5)$$

in which E_o is the elliptic integral of the second kind, and,

$$a = \frac{\pi^2}{32 E_o^2} \left[\left(\frac{b'}{a'}\right)^2 + 1 \right] \qquad (6\text{-}6)$$

where a' and b' are major and minor semi-axes of the ellipse respectively. β is equal to b'/a'.

F. Isosceles triangular ducts - The geometric constants for this shape of cross section are found to be given by

$$a + b = \frac{\frac{\tan\alpha \sin^2\alpha}{(1+\sin\alpha)^2}}{2\left\{ \frac{\tan\alpha}{3}\left(\frac{1}{\cos^2\alpha} - 1\right) + \sum_{n=1} 2\, C_n \frac{(2n-1)\pi}{2\alpha} + 2 \right\}^{-1} I_n}$$

and

$$a = \left\{ 4\left(\frac{1+\sin\alpha}{\sin\alpha}\right)^2 \left[\left(\frac{x}{b}\right)^2_{max} \left(\frac{1}{\cos^2\alpha} - 1\right) + \sum_{n=1} C_n \left(\frac{x}{b}\right)^{\frac{(2n-1)\pi}{2\alpha}}_{max} \right] \right\}^{-1}$$

where α = half opening angle of the duct

C_n = dimensionless constants, Table 1, Reference 39

I_n = integrals, Equation (12a) and Table 2, Reference 39

$(x/b)_{max}$ = value of x/b which gives the maximum value of the expression

$$u = \frac{a^2}{4\mu}\left(-\frac{dP'}{dx}\right)\left[\left(\frac{r}{a}\right)^2\left(\frac{1}{\cos 2\alpha} - 1\right) + \sum_{n=1} C_n \left(\frac{r}{a}\right)^{\frac{(2n-1)\pi}{2\alpha}}\right]$$

a = height of the isosceles duct

The values of a and b determined using the above expressions are shown in Figures 1, 2, 3, and 4, and tabulated in Appendix II.

VII - COMPARISON

Comparisons have been made with the available data and classified according to the cross-sectional geometries.

A. Pipes and Parallel Plates

Metzner and Reed (37) have correlated the available data on flow of non-Newtonian fluids in pipes in a fashion analogous to the conventional friction factor-Reynolds number plot for Newtonian fluids. Their correlation, theoretically rigorous in the laminar region, was tested with data on 16 different non-Newtonian materials. Their generalized Reynolds number is

$$N_{Re'} = \frac{D^{n'} U^{2-n'} \rho}{\gamma} \tag{7-1}$$

where

$$\gamma = g_c K' 8^{n'-1} \tag{7-2}$$

The friction factor - Reynolds number relationship can be obtained by substitution of the value for $\frac{D}{4}(-dP'/dx)$, which for tube flow data is equal to $K'(8U/D)^{n'}$, into the definition of the friction factor

$$f = \frac{\frac{D}{4}\left(-\frac{dP'}{dx}\right) g_c}{\frac{1}{2}\rho U^2}$$

$$= \frac{K'\left(\frac{8U}{D}\right)^{n'} g_c}{\frac{1}{2}\rho U^2} \tag{7-3}$$

$$= \frac{16}{N_{Re'}}$$

Christiansen, Ryan, and Stevens (43) have published some pipe flow data and a graph for predicting non-Newtonian tube flow. In Table 2 of their paper, the percentage mean deviations from the observed data for one case (15% Napalm in Kerosene through 1-1/2 in. pipe) are 3.1 when using the Powell-Eyring model and 5.4 when using power law model.

Perkins and Click (44) rearranged the Buckingham-Reiner equation and obtained a relation in terms of dimensionless groups.

$$\frac{1}{N_{Re}} = \frac{f}{16} - \frac{1}{6}\frac{N_{He}}{(N_{Re})^2} + \frac{1}{3}\frac{N_{He}^4}{f^3 (N_{Re})^8} \qquad (7\text{-}4)$$

where $N_{He} = \frac{\tau_y D^2 \rho g_c}{\beta^2}$, the extensive data of Govier and Winning (45) on the plot using N_{He} as a parameter supports the conclusion that the transition from laminar to turbulent flow occurs at progressively higher Reynolds numbers as the Hedstrom number increases.

Data for flow between parallel plates have not been found. However, it may be expected that similar results can be obtained since the deduction of flow rate and pressure loss from the equation of motion and a fluid model is analogous to tube flow.

The above comparisons were made between rigorous derivations and the experimental data. It is not necessary to discuss the equations proposed by the present work, since they are identical with the equations derived rigorously for flow through tubes and between parallel plates.

B. Annuli

There is no experimental data available for non-Newtonian flow through annuli. The analytical and numerical solutions reported by Fredrickson and Bird (9) have been used for comparison.

For power law fluids, the following equivalent quantities may be obtained from the published solution and the proposed equation.

$$\frac{2U/v_{max}}{\left(-r_w \frac{dP'}{dz}/K\right)^{\frac{1}{n}}} = \frac{4\gamma n}{(1+n)(1+2n)} \qquad (7\text{-}5)$$

$$\gamma = \gamma(n, k)$$

$$\gamma(n, 0) = \frac{1+2n}{1+3n}$$

$$\gamma(n, 1) = 1$$

The numerical values of γ are tabulated in Reference (9). The proposed equation is

$$\frac{2U/v_{max}}{\left(-r_w \frac{dP'}{dz}/K\right)^{\frac{1}{n}}} = \frac{n}{a+bn} \qquad (7\text{-}6)$$

which may be rearranged to give

$$\frac{-r_H \frac{dP'}{dx}/K}{(2U/r_H)^n n^{-n}} = (a + bn)^n \qquad (7\text{-}7)$$

The maximum velocities have been compared by consideration of the ratio of maximum velocity to the average velocity. Values of this ratio are tabulated in the cited reference. The predicted expression is

$$\frac{u_{max}}{U} = \frac{1 + \frac{b}{a} n}{1 + n} \qquad (7\text{-}8)$$

For Bingham flow through annuli, Fredrickson and Bird (9) give the following solution:

$$\frac{2U/r_H}{-r_H \frac{dP'}{dx}/\beta} = \frac{\Omega_B}{(1 - k^2)(1 - k)^2} \qquad (7\text{-}9)$$

The proposed solution is

$$\frac{2U/r_H}{-r_H \frac{dP'}{dx}/\beta} = \frac{1}{a + b} - \frac{1}{b}\left(\frac{T_1}{1 - k}\right) + \frac{a}{(a + b)b}\left(\frac{T_1}{1 - k}\right)^{\frac{b}{a} + 1} = c_B \qquad (7\text{-}10)$$

The analytically determined expression for u_{max}/U is

$$\frac{u_{max}}{U} = \frac{4\beta_o(1 - k^2)}{\Omega_B} \qquad (7\text{-}11)$$

where the values of β_o and Ω_B have also been in Table 1, Reference 9. The maximum to average velocity ratio predicted by the method of Konicki is

$$\frac{u_{max}}{U} = \frac{1 - 2\left(\frac{T_1}{1-k}\right) + \left(\frac{T_1}{1-k}\right)^2}{2a\left[\frac{1}{a+b} - \frac{1}{b}\left(\frac{T_1}{1-k}\right) + \frac{a}{(a+b)b}\left(\frac{T_1}{1-k}\right)^{\frac{b}{a}+1}\right]} \qquad (7\text{-}12)$$

For Rabinowitsch fluids, the dimensionless velocity yielded by Rotem (10) is

$$\frac{2U/\varepsilon_H}{-\varepsilon_H \frac{dP'}{dx}/\mu_o} = \frac{8\Omega}{(1-k^2)(1-k)^2} \qquad (7\text{-}13)$$

while the present method yields

$$\frac{2U/\varepsilon_H}{-\varepsilon_H \frac{dP'}{dx}/\mu_o} = \frac{1}{a+b} + \frac{C_1(1-k)^2}{b+3a} \qquad (7\text{-}14)$$

where $\Omega = \Omega(C_1, k)$ Eq. 12, Ref. 10

$$C_1 = b_1\left(\frac{-\varepsilon_H \frac{dP'}{dx}}{1-k}\right)^2$$

b_1, μ_o = parameters in the Rabinowitsch fluid model.

Values of dimensionless velocities, dimensionless pressure losses, and u_{max}/U are tabulated in Appendix III, Table 1 through 5. Percentage errors are also reported in these tables.

Plots of these data are given in Figures 5 through 12.

C. Rectangular Ducts

Schechter's solution (18) for power law flow in rectangular ducts is

$$\frac{2U/r_H}{(-r_H \frac{dP'}{dx}/K)^{\frac{1}{n}}} = \left[\frac{(4(1+E)/E)^{n+1}}{N_{Re}'' f} \right]^{\frac{1}{n}} \qquad (7\text{-}15)$$

The predicted relationship is

$$\frac{2U/r_H}{(-r_H \frac{dP'}{dx}/K)^{\frac{1}{n}}} = \frac{n}{a+bn} \qquad (7\text{-}16)$$

In Eq. (7-15), E is the aspect ratio. The values of $N_{Re}'' f$ have been reported in Table 3, Ref. 18. Some values of $N_{Re}'' f$ obtained by another approach (19) have also been used in the comparison. The ratio of maximum velocity to average velocity (18) is

$$\frac{u_{max}}{U} = \sum_{i=1}^{6} a_i \sin \frac{c_i}{2} \sin \frac{\beta_i E}{2} \qquad (7\text{-}17)$$

while the prediction gives

$$\frac{u_{max}}{U} = \frac{1+\frac{b}{a}n}{1+n} \qquad (7\text{-}18)$$

where values of c_i, a_i and β_i are given in Table 3 and Table 2, Ref. 18.

Results of the comparison are given in Figures 13, 14, and 15. Numerical values are tabulated in Tables 8 through 12, Appendix III.

D. Elliptical Ducts

The dimensionless bulk velocity for power law flow through elliptic ducts as determined by Mizushina, Mitsuishi and Nakamura (20) is given by

$$\frac{2U/v_H}{(-v_H \frac{dP'}{dx}/K)^{\frac{1}{n}}} = \frac{2n}{3n+1} \left(\frac{1}{H'}\right)^{\frac{1}{n}} \left(\frac{4E_e}{\pi}\right)^{\frac{n+1}{1}} \qquad (7\text{-}19)$$

where E_e is the elliptic integral of the second kind and

$$H' = H'(\beta, n)$$

$$\beta = b'/a'$$

compared with the current expression

$$\frac{2U/v_H}{(-v_H \frac{dP'}{dx}/K)^{\frac{1}{n}}} = \frac{n}{a+bn} \qquad (7\text{-}20)$$

The ratio of maximum to average velocity determined by the above authors is

$$\frac{u_{max}}{U} = \frac{1+3n}{1+n} \qquad (7\text{-}21)$$

The predicted expression for this ratio is

$$\frac{u_{max}}{U} = \frac{1 + \frac{b}{a} n}{1 + n} \qquad (7\text{-}22)$$

Since b/a for elliptic ducts is equal to 3 for all values of β, it is seen that Eq. (7-21) and Eq. (7-22) yield the same result in this instance. The results of comparison are shown in Figs. 16 and 17. Numerical values are given in Tables 13 and 14, Appendix III.

E. Isosceles Triangular Ducts

Values of a and b were determined for cross-sections having this geometry from Newtonian flow data. However, no non-Newtonian flow data is available for comparison purposes.

Percentage Error

The percentage error reported in the tables has been defined as follows:

$$\% \text{ Error} = \frac{\text{predicted value} - \text{other authors' value}}{\text{other authors' value}} \times 100 \qquad (7\text{-}23)$$

All the errors listed in the appendix were evaluated before rounding off to the correct number of significant figures in the calculated quantities.

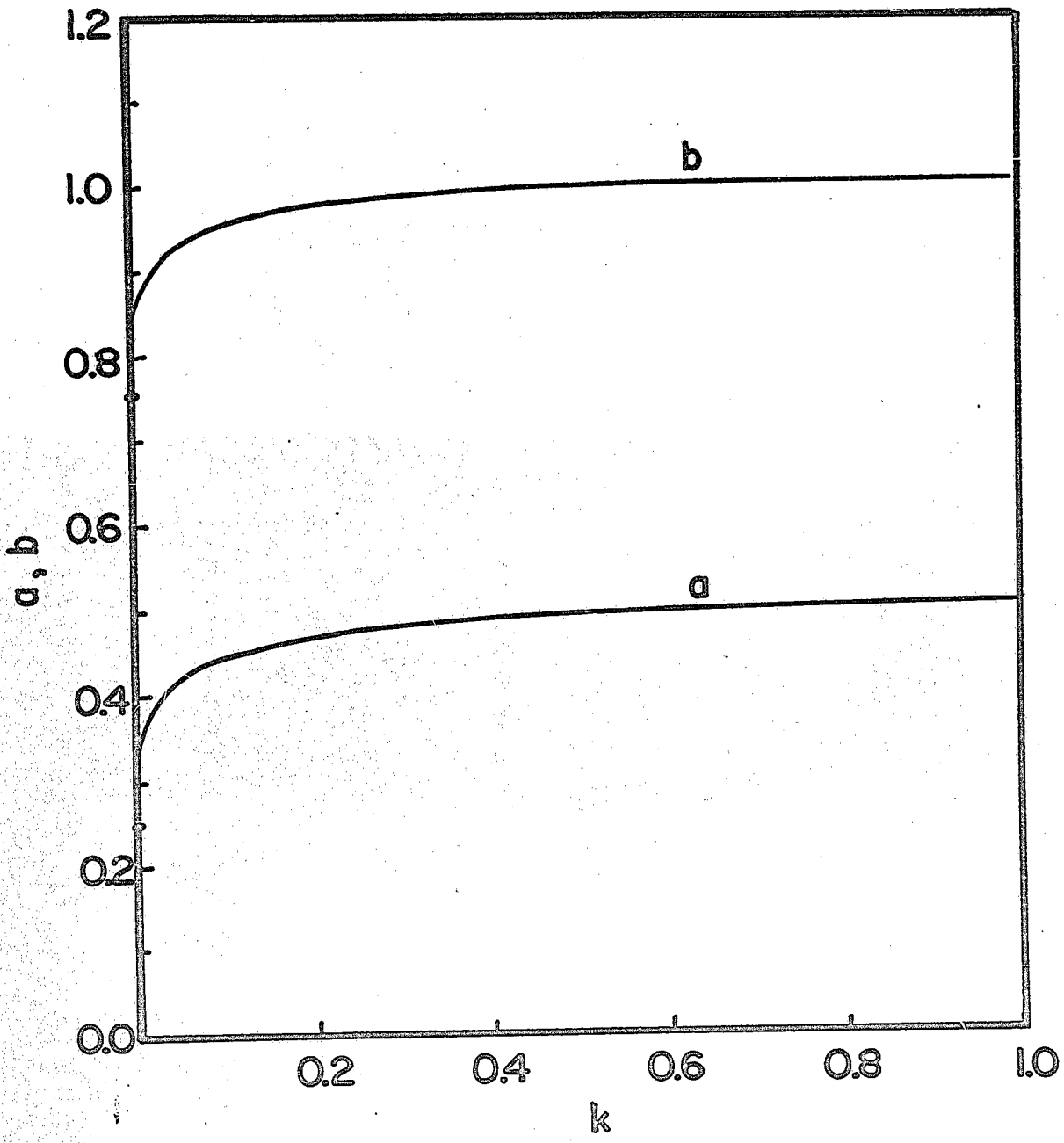

Figure 1. PLOT OF GEOMETRIC CONSTANTS FOR CONCENTRIC ANNULI AS A FUNCTION OF k

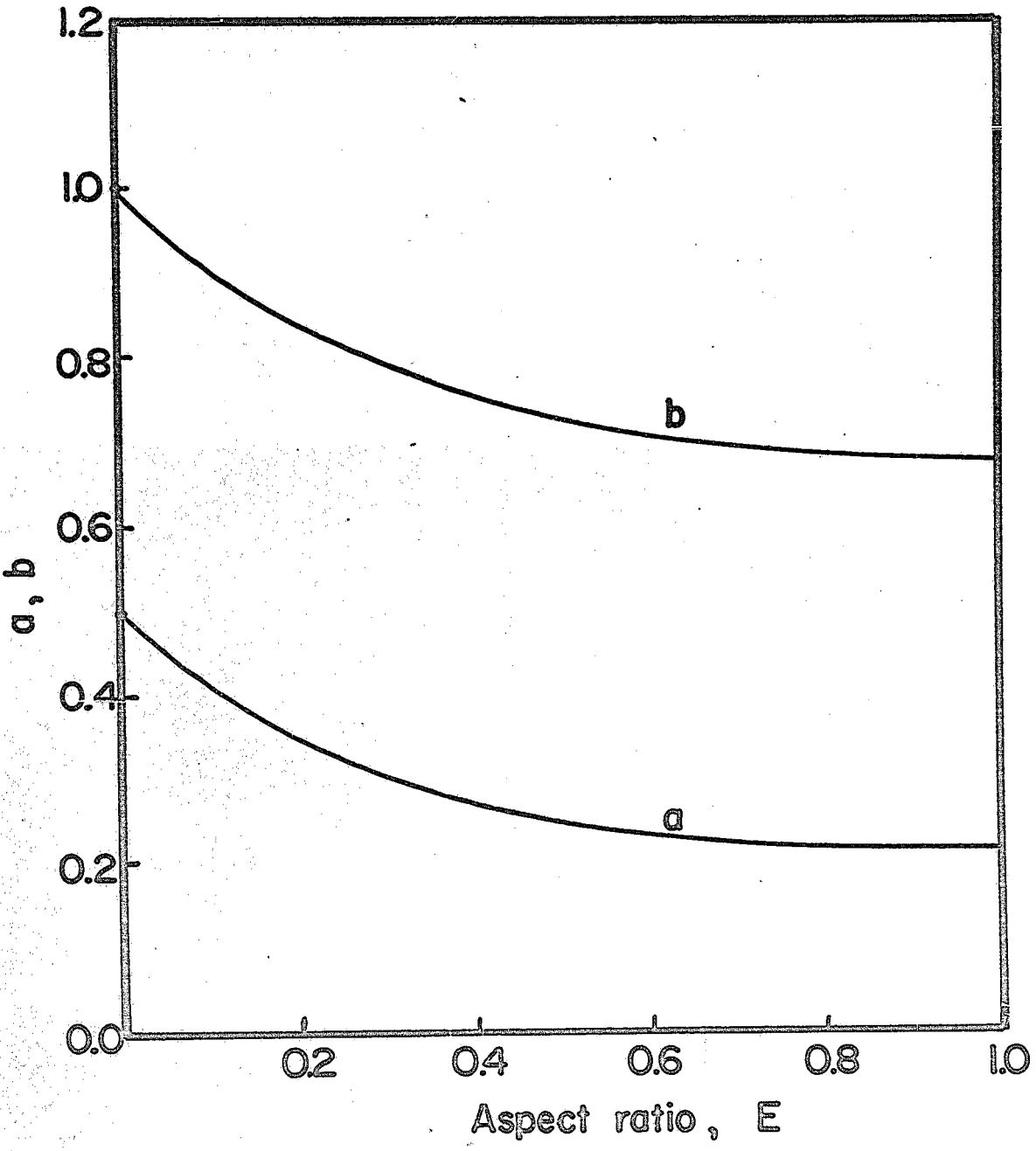

Figure 2. PLOT OF GEOMETRIC CONSTANTS FOR RECTANGULAR DUCTS AS A FUNCTION OF ASPECT RATIO

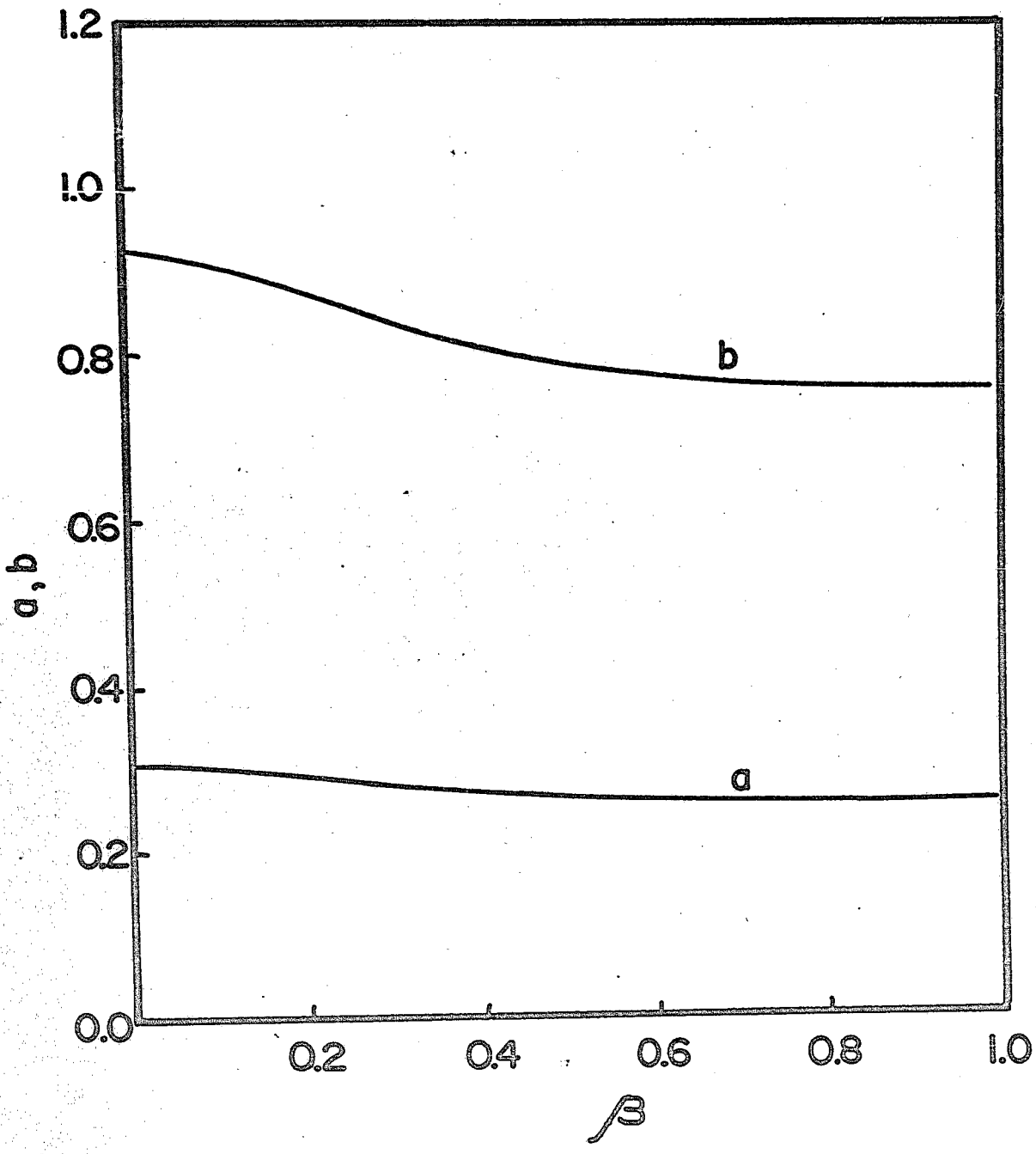

Figure 3. PLOT OF GEOMETRIC CONSTANTS FOR ELLIPTIC DUCTS AS A FUNCTION OF β

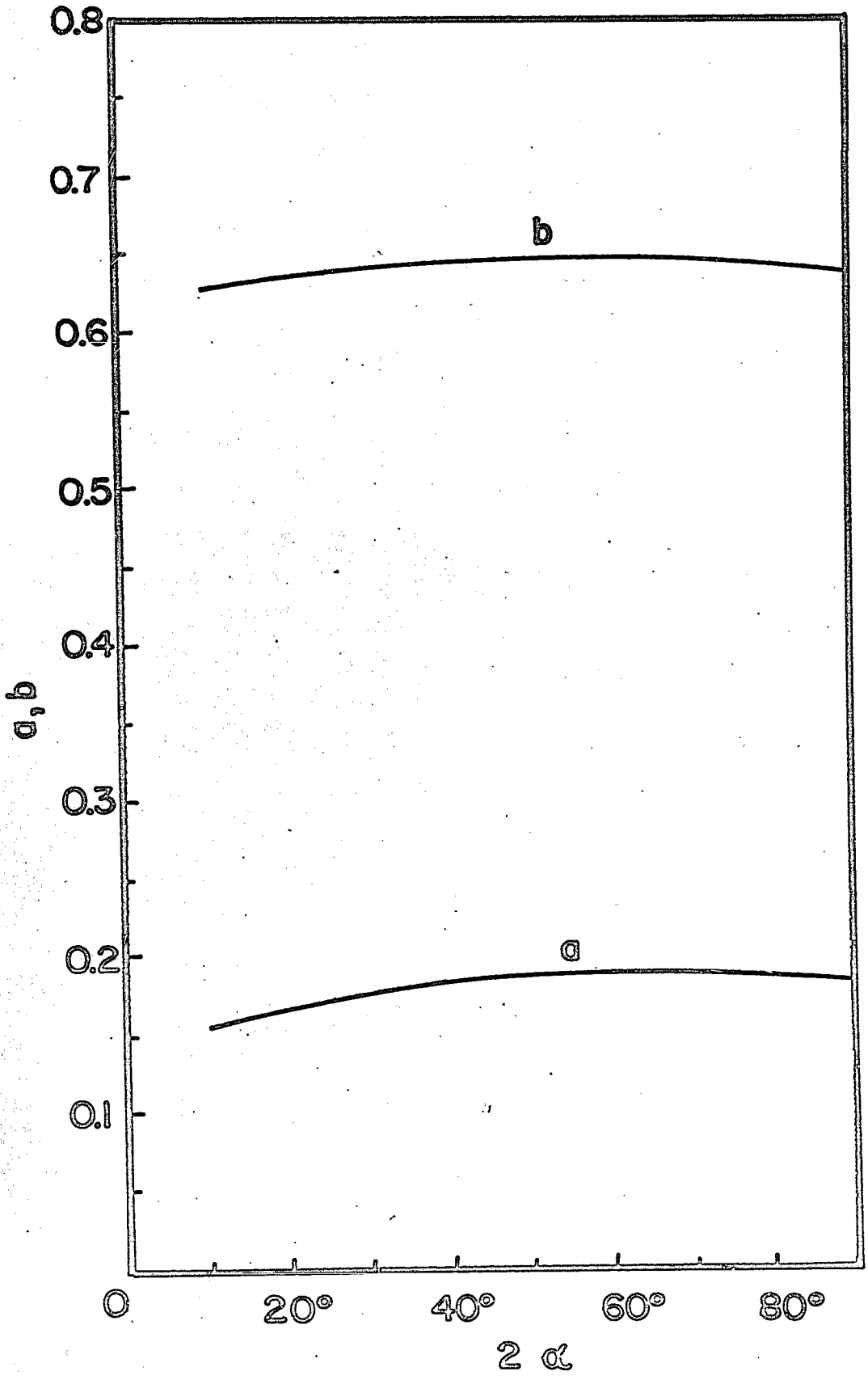

Figure 4. PLOT OF GEOMETRIC CONSTANTS FOR ISOSCELES TRIANGULAR DUCTS AS A FUNCTION OF α

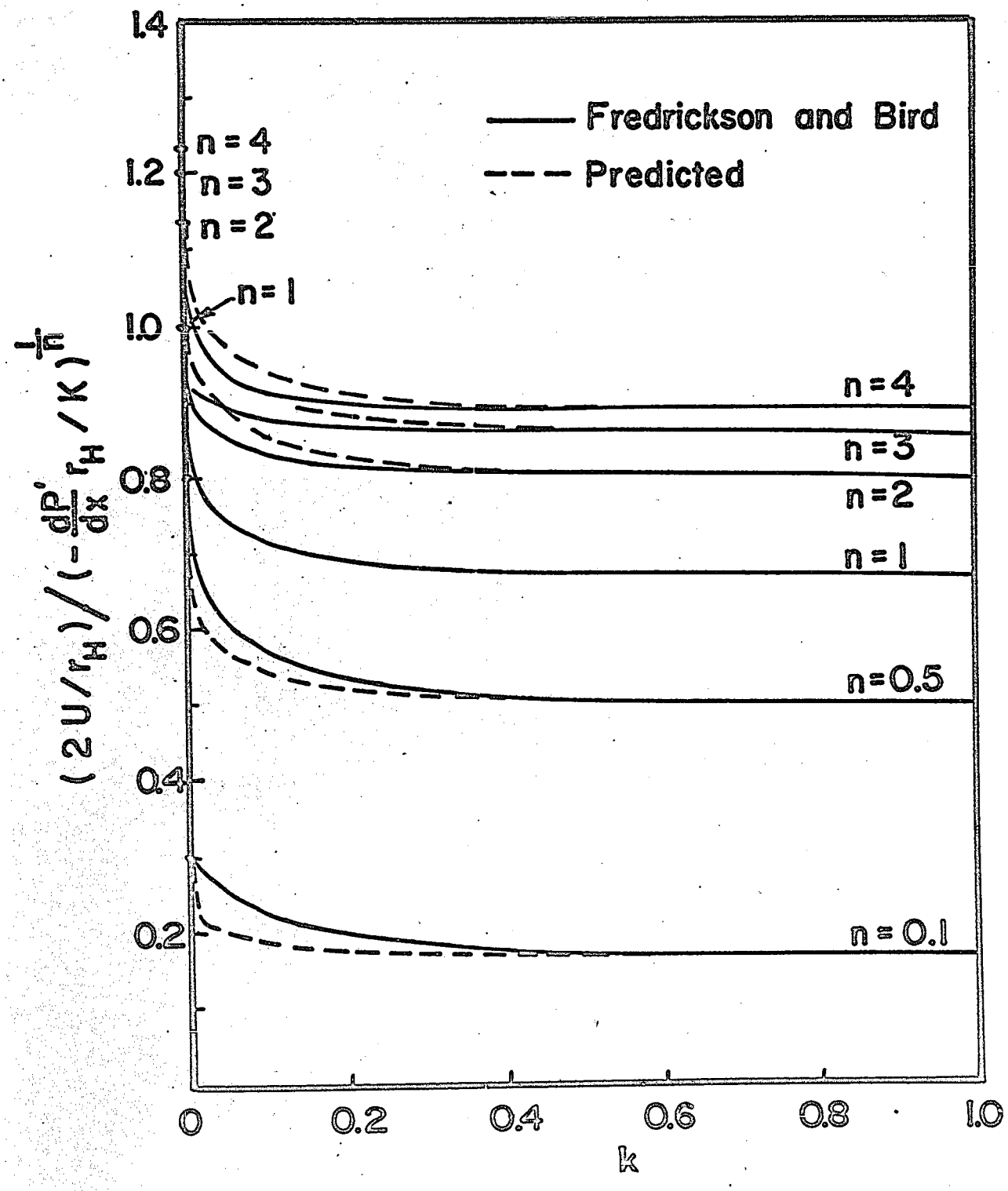

Figure 5. COMPARISON OF DIMENSIONLESS VELOCITY FOR POWER LAW FLOW THROUGH CONCENTRIC ANNULI

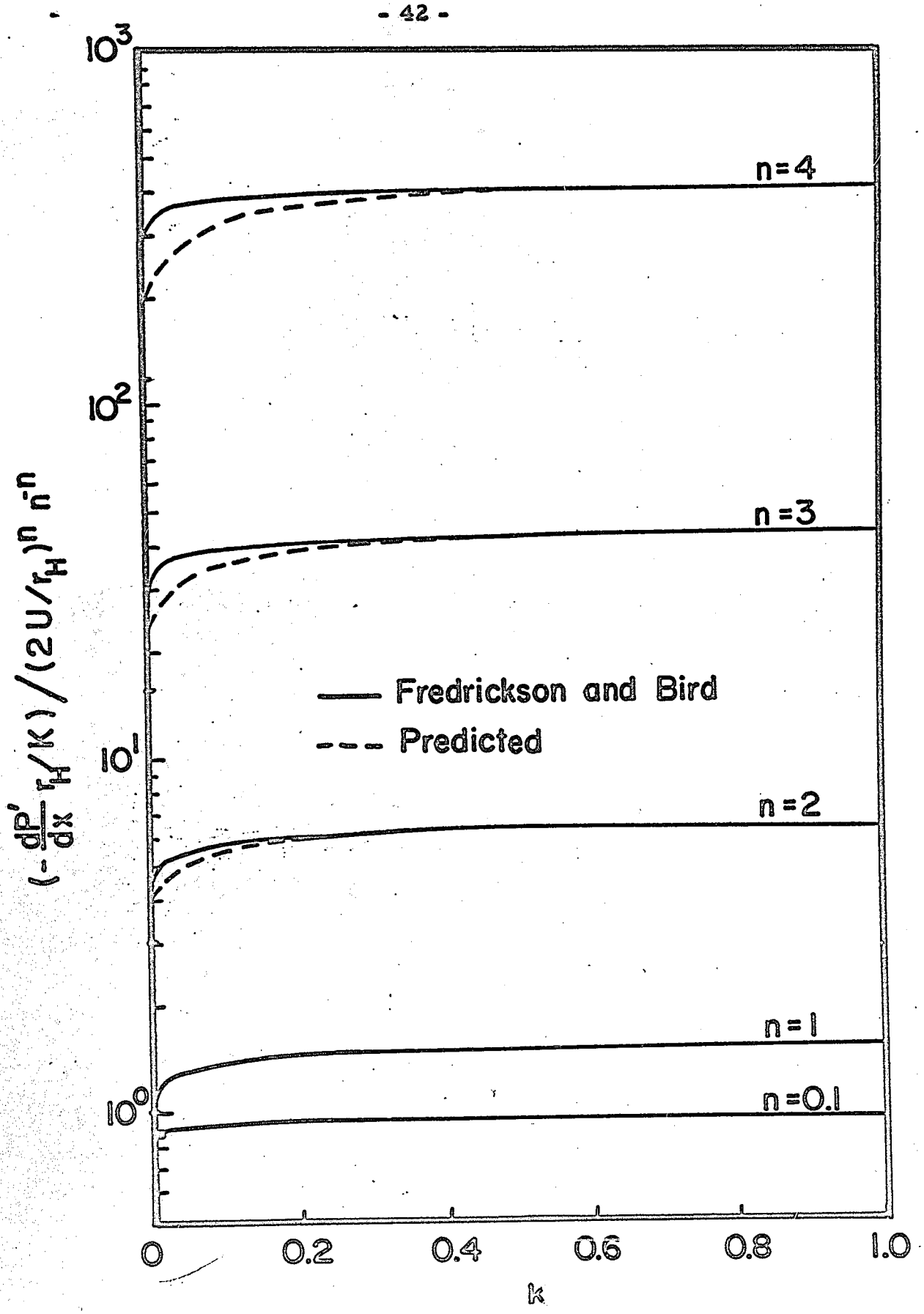

Figure 6. COMPARISON OF DIMENSIONLESS PRESSURE DROP FOR POWER LAW FLOW THROUGH CONCENTRIC ANNULI

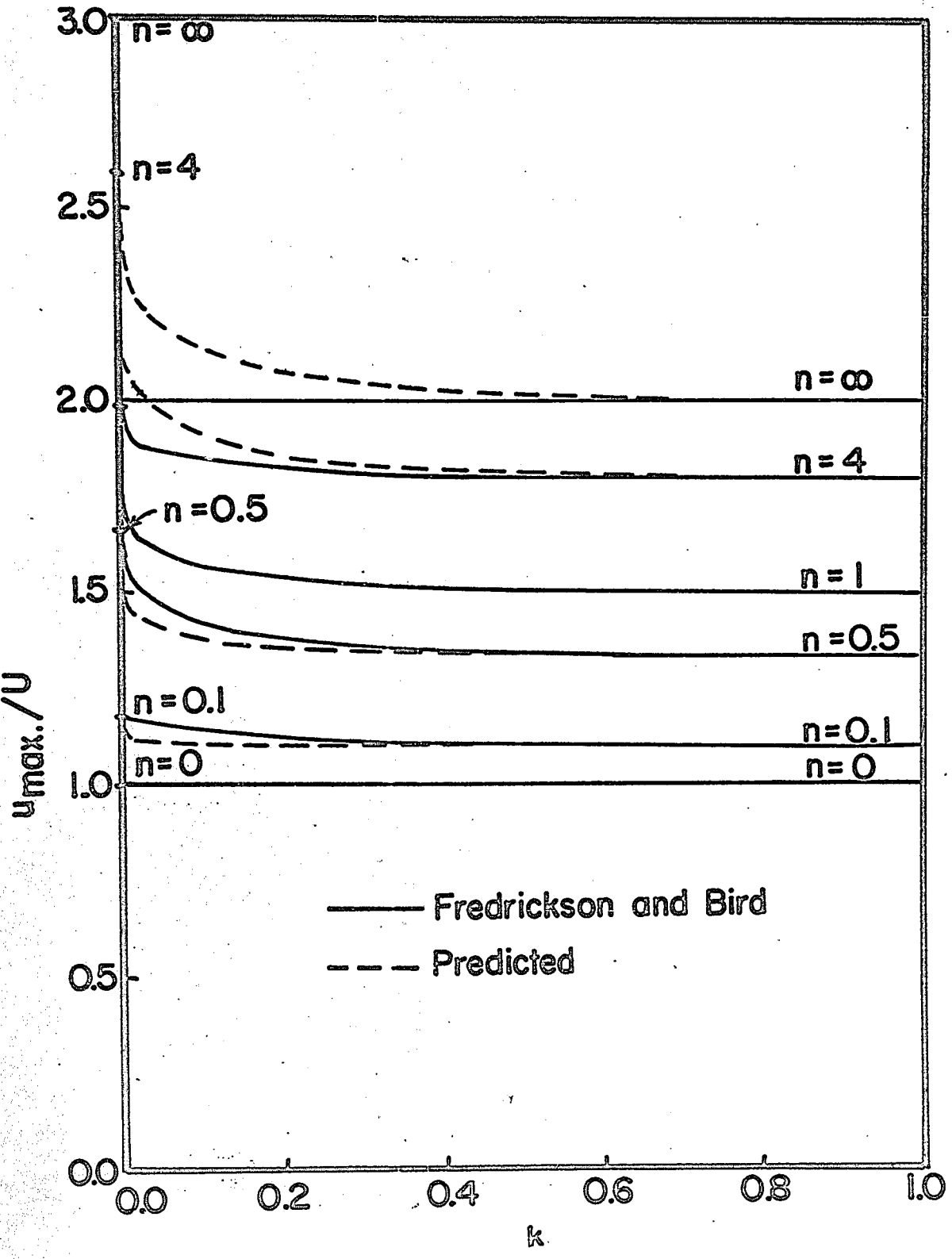

Figure 7. COMPARISON OF $u_{max.}/U$ FOR POWER LAW FLOW THROUGH CONCENTRIC ANNULI

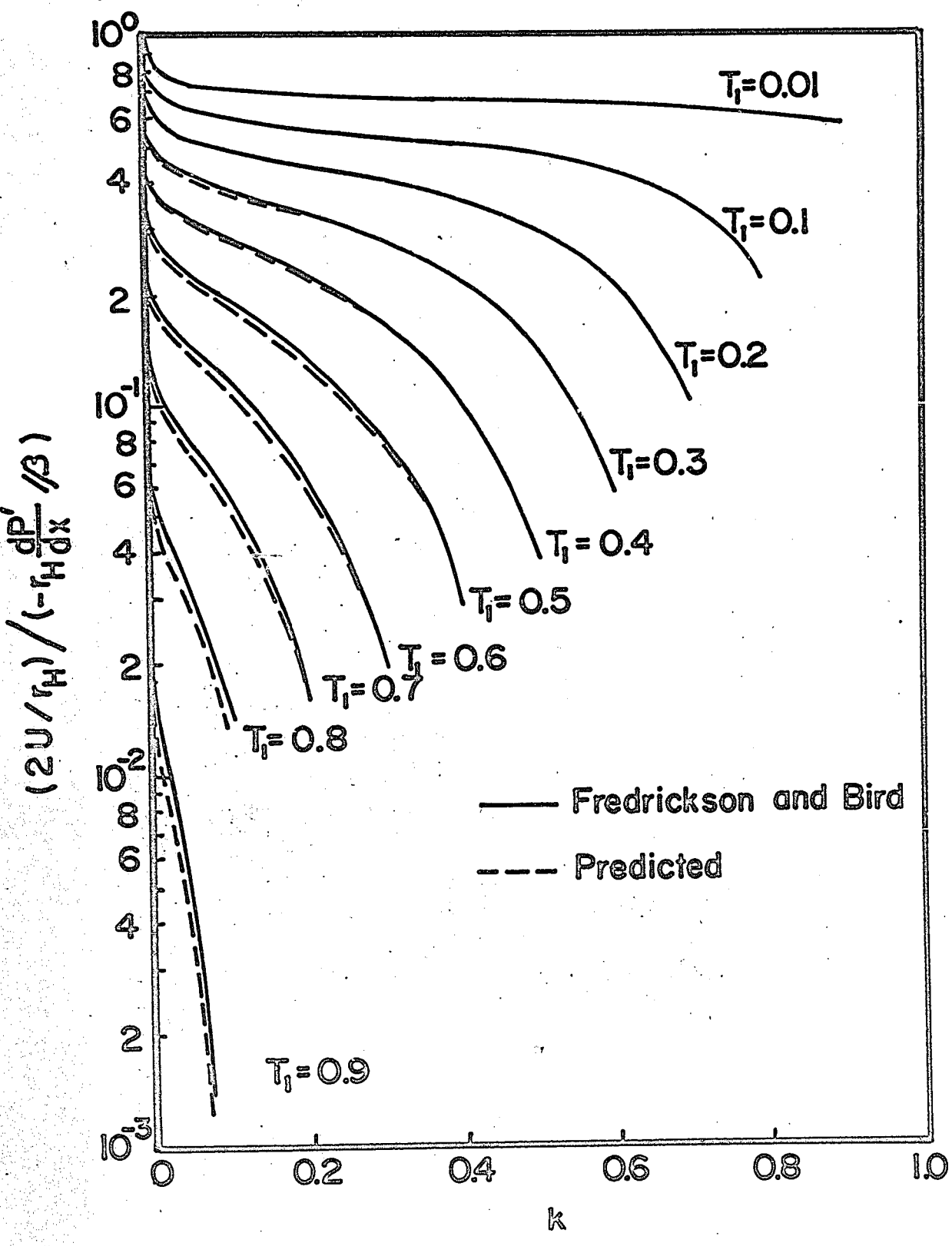

Figure 8. COMPARISON OF DIMENSIONLESS VELOCITY FOR BINGHAM FLOW THROUGH CONCENTRIC ANNULI

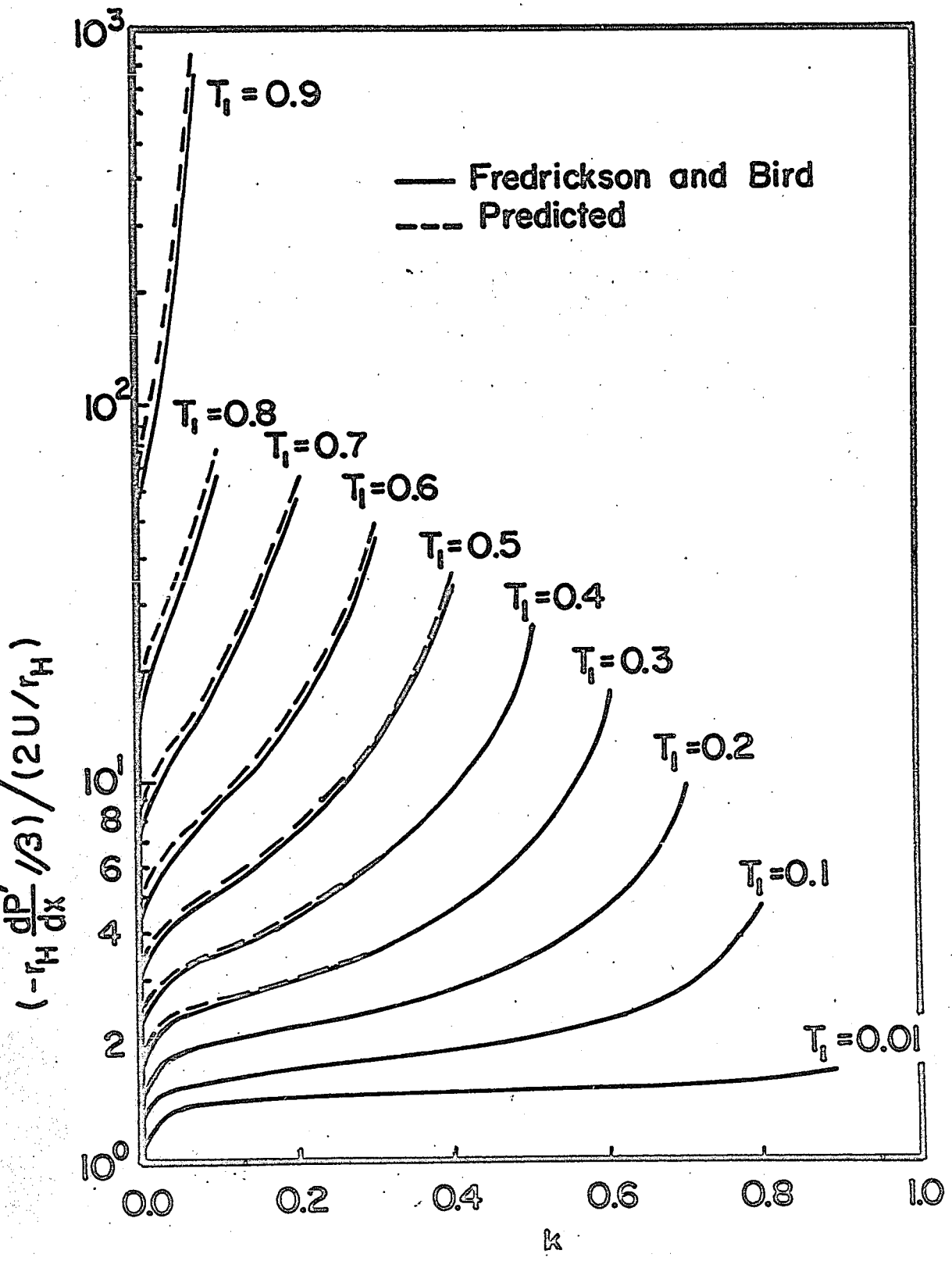

Figure 9. COMPARISON OF DIMENSIONLESS PRESSURE DROP FOR BINGHAM FLOW THROUGH CONCENTRIC ANNULI

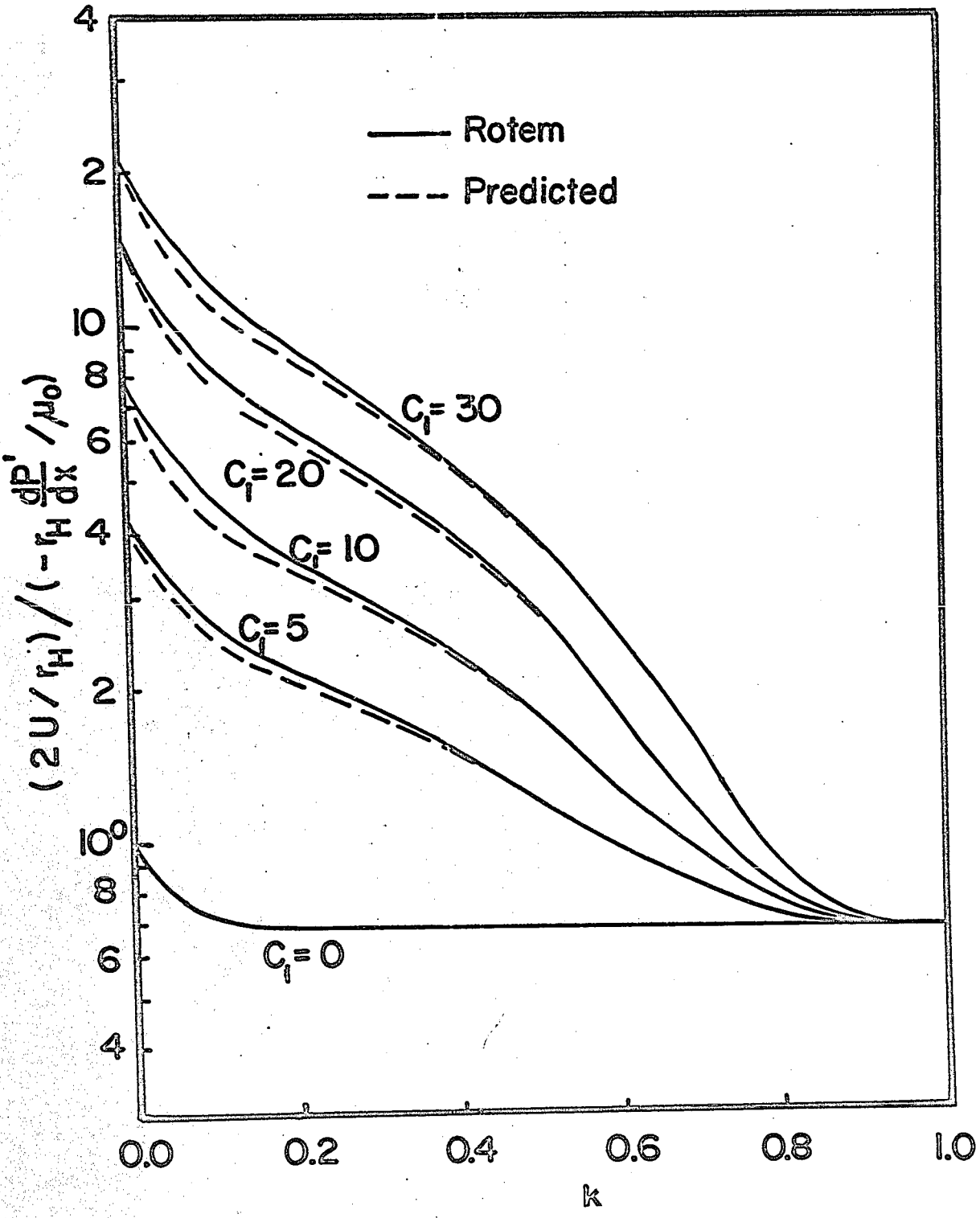

Figure 11. COMPARISON OF DIMENSIONLESS VELOCITY FOR RABINOWITSCH FLOW THROUGH ANNULI

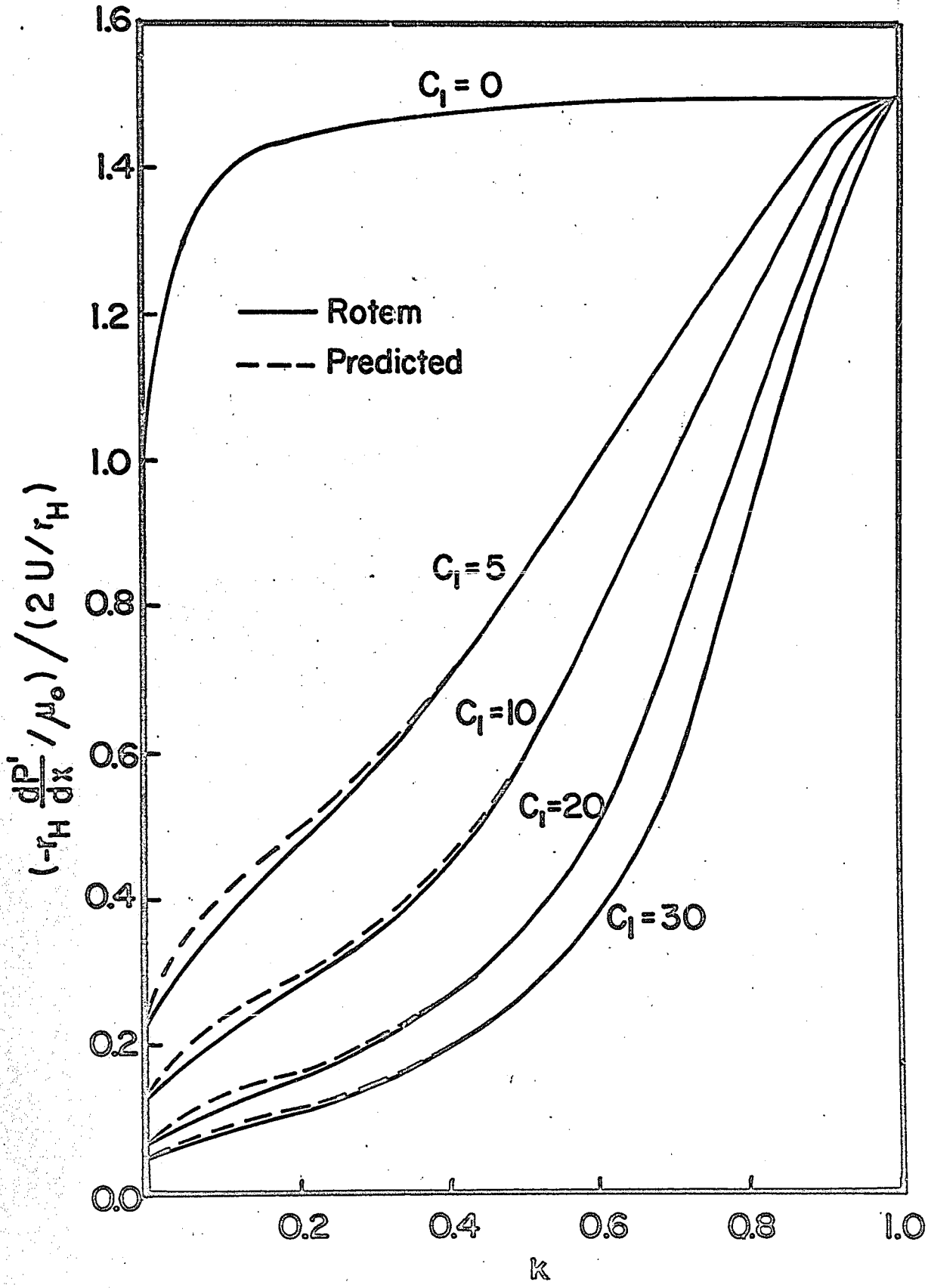

Figure 12. COMPARISON OF DIMENSIONLESS PRESSURE DROP FOR RABINOWITSCH FLOW THROUGH ANNULI

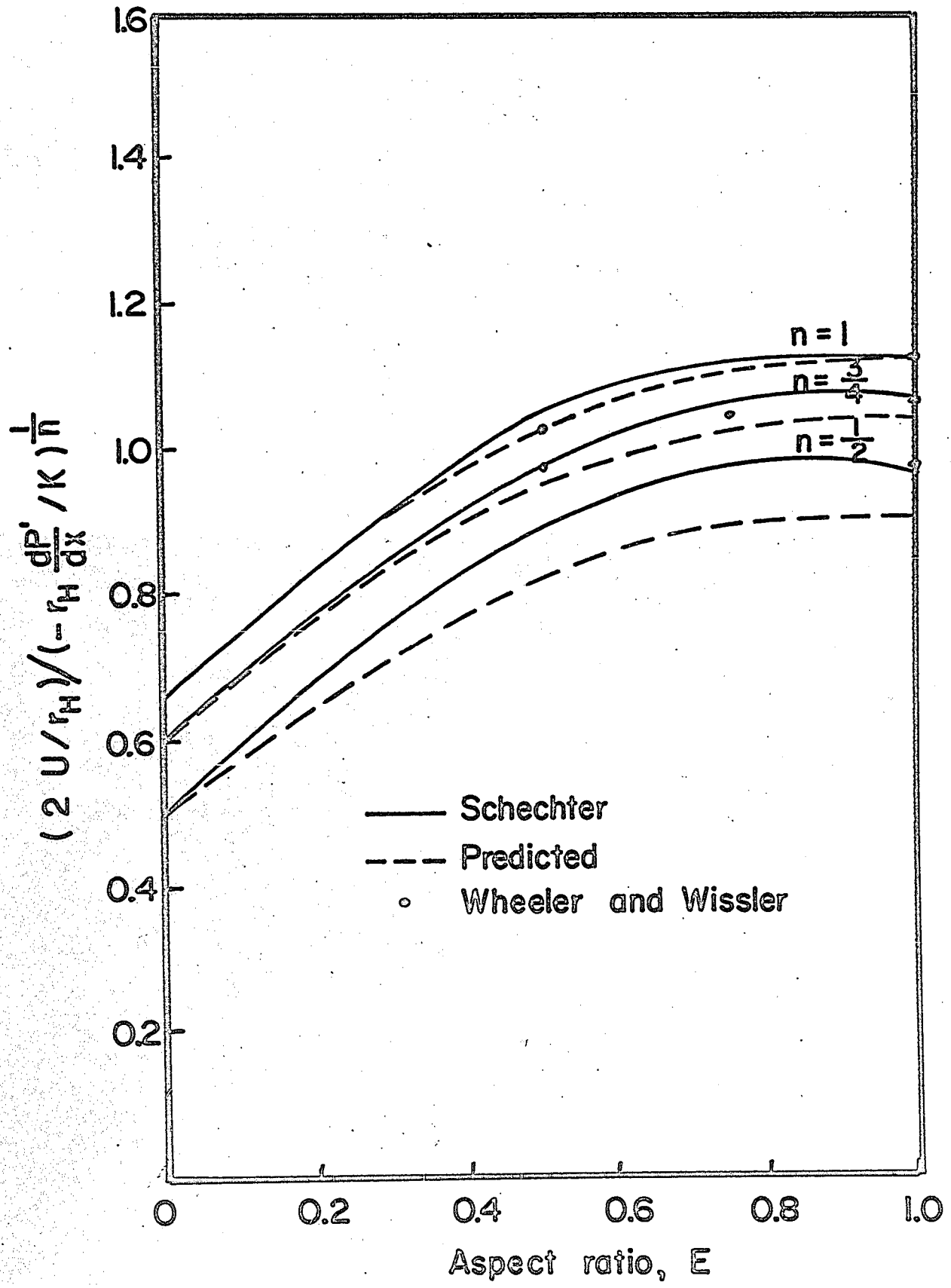

Figure 13. COMPARISON OF DIMENSIONLESS VELOCITY FOR PSEUDOPLASTIC FLOW THROUGH RECTANGULAR DUCTS

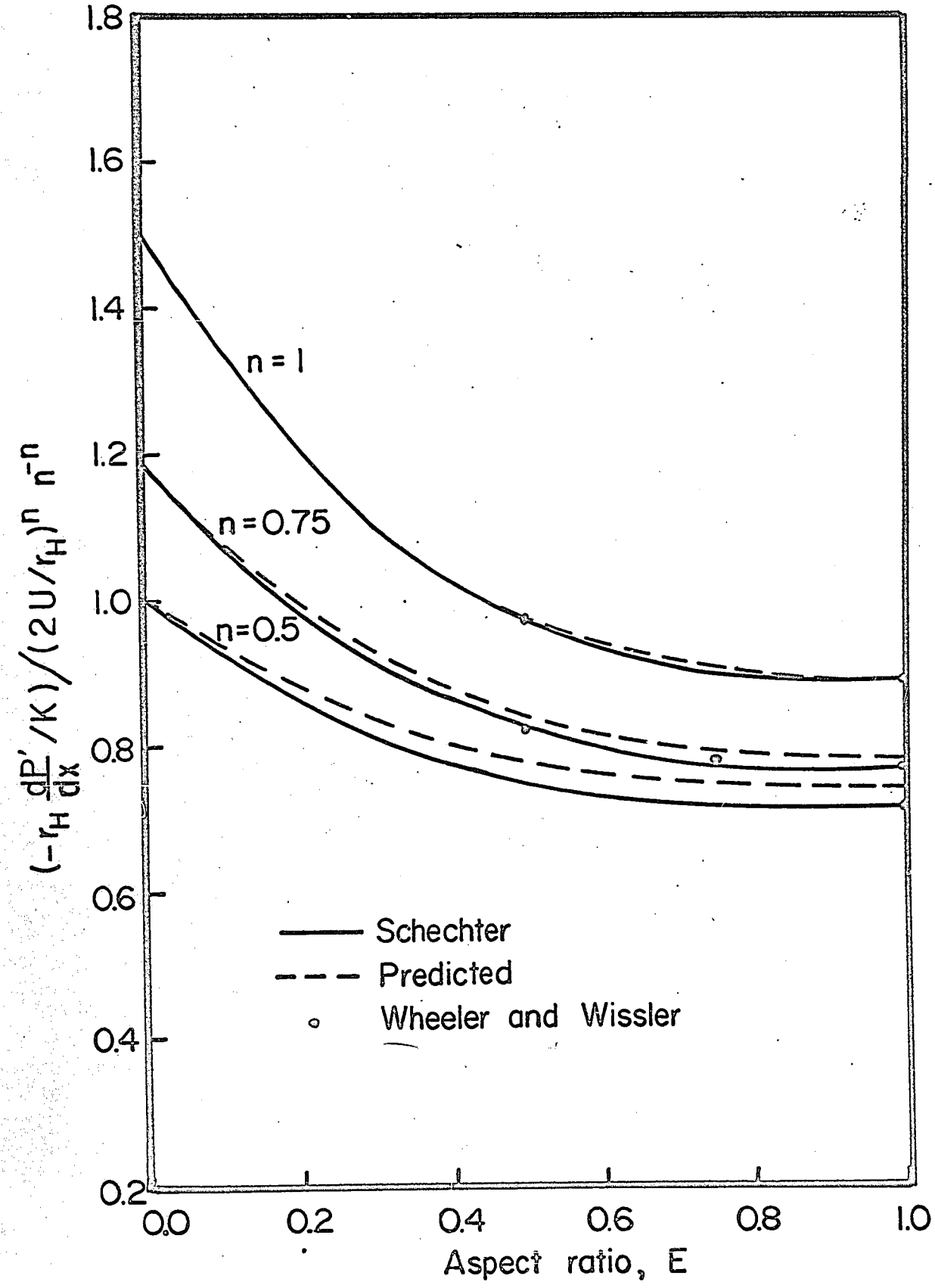

Figure 14. COMPARISON OF DIMENSIONLESS PRESSURE DROP FOR PSEUDOPLASTIC FLOW THROUGH RECTANGULAR DUCTS

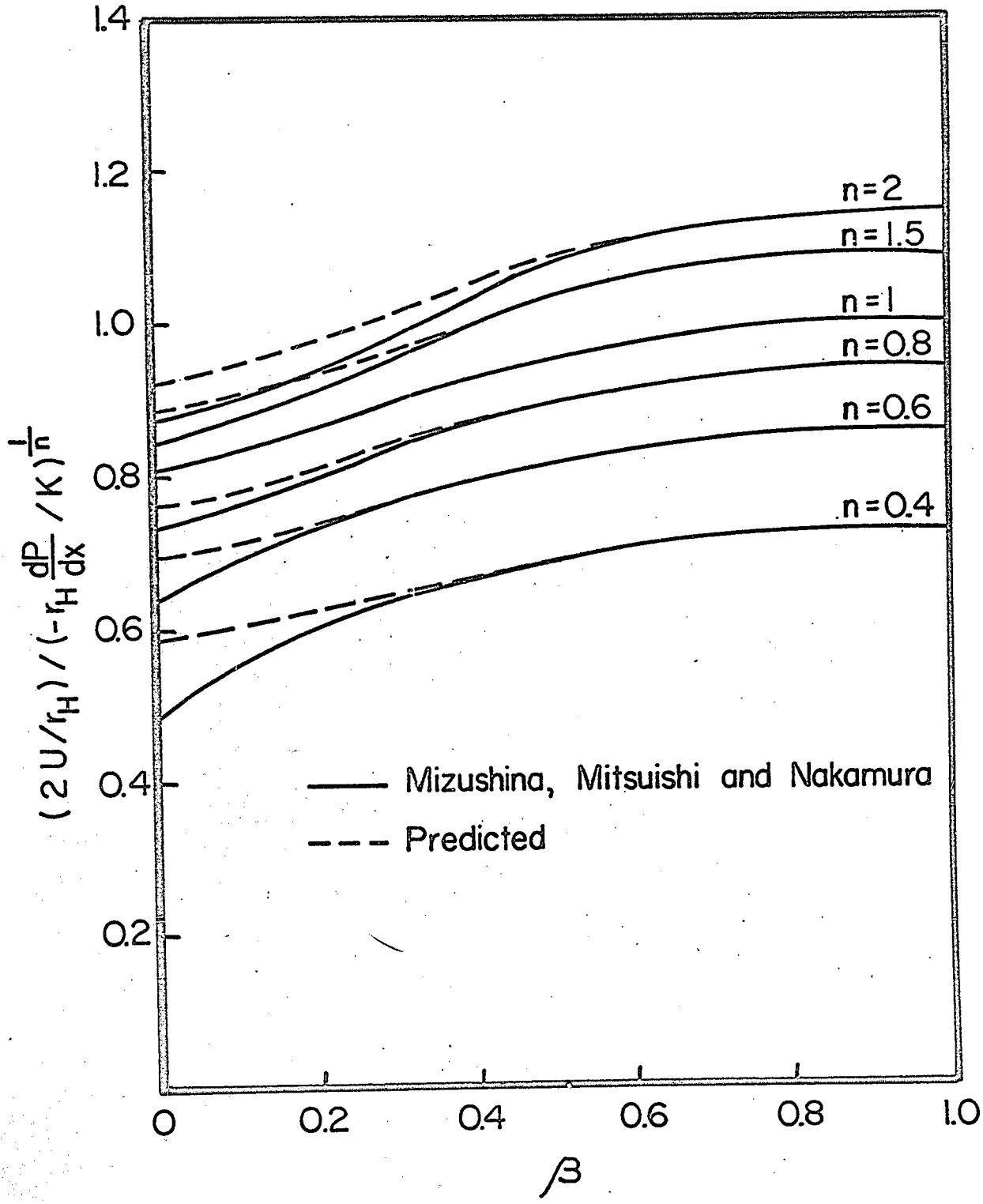

Figure 16. COMPARISON OF DIMENSIONLESS VELOCITY FOR POWER LAW FLOW THROUGH ELLIPTIC DUCTS

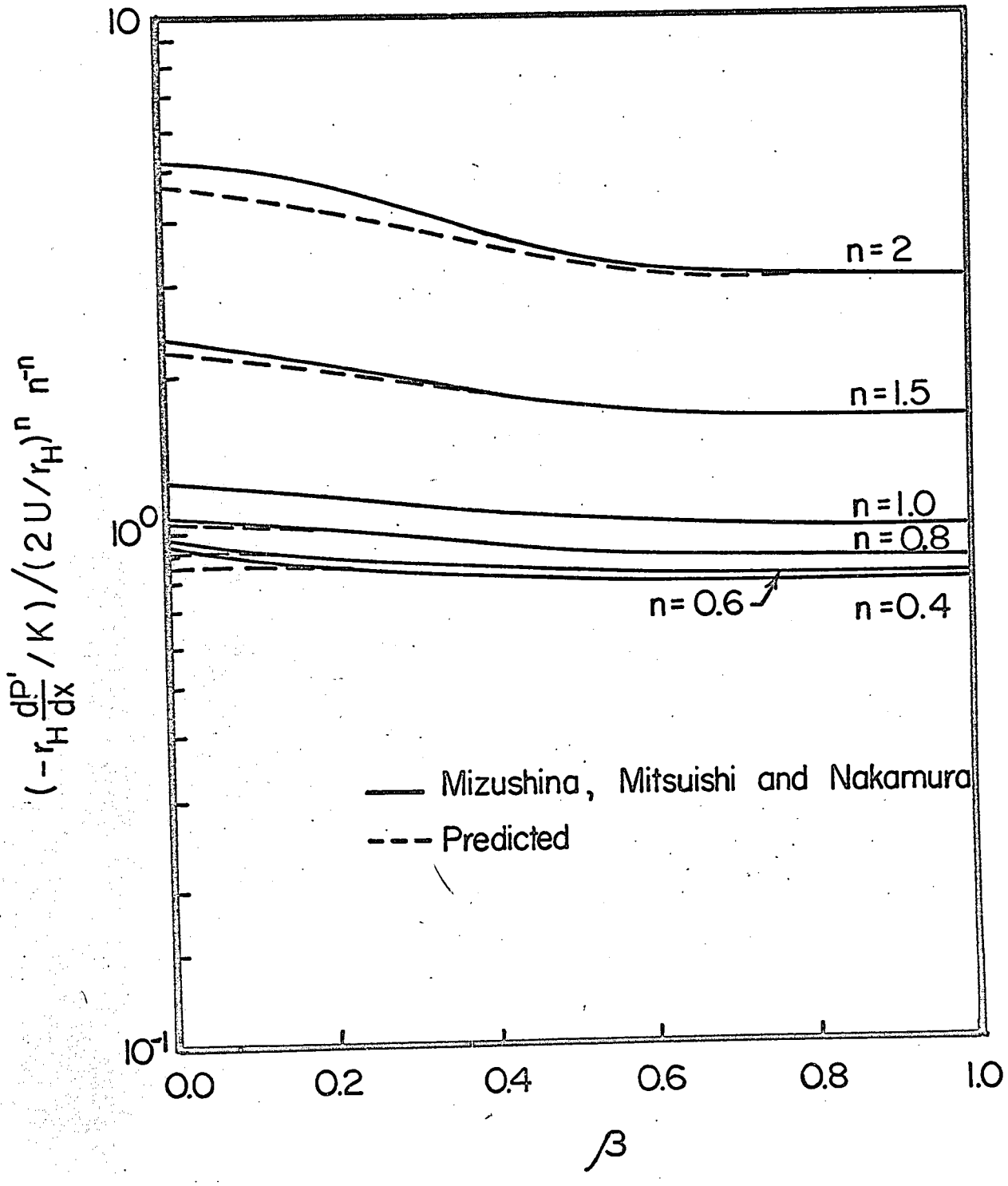

Figure 17. COMPARISON OF DIMENSIONLESS PRESSURE DROP FOR POWER LAW FLOW THROUGH ELLIPTIC DUCTS

VIII - DISCUSSION AND CONCLUSION

It should be emphasized that all the results obtained by the present method are exact for flows through circular tubes and parallel plates, as well as for Newtonian flows through any shape of cross sections. The agreement in other situations between the predicted values and those obtained by rigorous analysis in general may be considered good enough for design purposes.

For the flow of power law fluids through annuli, the errors involved in prediction of the pressure drops and bulk velocities are less than 5 per cent for value of n ranging from 0.1 to 4 and k in the range from 0.4 to 1. In the case of Bingham flow through annuli, the errors are less than 3 per cent for all T_1 and for k values in the range from 0.3 to 1. In the flow of Rabinowitsch fluids through annuli, for C_2 values ranging from 0. to 30 and k from 0.2 to 1, the errors involved are within 5 per cent. The deviations become very large for small values of k. For example, the maximum error in bulk velocity prediction which occurs at k = 0.01, n = 4 for power-law fluids, is 24.75 per cent. The dependence of error on geometry might be explained in the following way: In the rigorous derivations, the calculations often involve a shear stress distribution which is different for various fluids. For example, the zero shear stress position for power law fluid flow through an

eliminating expensive and elaborate experimental work for those problems which have not been solved to arrive at a reliable result well within engineering accuracy.

IX - RECOMMENDATION

In the determination of the values of a and b for other arbitrary cross sections not included in the present work, two measurements are sufficient, i.e., the average velocity and maximum velocity for a Newtonian fluid. The method may also be applied to flow in open-channel and through packed beds. In fact, Tia (40) has extended the generalized Rabinowitsch-Mooney equation to the flow of fluids through porous media, and is currently investigating open-channel flow.

APPENDIX I

Fluid Models and Bulk Velocity Expressions

A. The Fluid Models

1. The Bingham Model

$$\tau_{yx} = -\beta \frac{dv_x}{dy} \pm \tau_y \quad \text{if} \quad |\tau_{yx}| > \tau_y$$

$$\frac{dv_x}{dy} = 0 \quad \text{if} \quad |\tau_{yx}| < \tau_y$$

2. The Ostwald-de Waele (Power-law) Model

$$\tau_{yx} = -K \left(\frac{dv_x}{dy}\right)^{n-1} \frac{dv_x}{dy}$$

3. The Eyring Model

$$\tau_{yx} = A \operatorname{arcsinh}\left(-\frac{1}{B}\frac{dv_x}{dy}\right)$$

4. The Ellis Model

$$-\frac{dv_x}{dy} = \left(\psi_0 + \psi_1 \left|\tau_{yx}\right|^{\alpha-1}\right)\tau_{yx}$$

5. The Reiner-Philippoff Model

$$-\frac{dv_x}{dy} = \left(\frac{1}{\mu + \dfrac{\eta_0 - \mu}{1 + (\tau_{yx}/\tau_0)^2}}\right)\tau_{yx}$$

6. The Prandtl-Eyring Model

$$\frac{dv_x}{dy} = \frac{1}{\eta_0}\left(\tau_{yx} + b_1 \tau_{yx}^3\right)$$

B. The Bulk Velocity Expressions

1. For the Bingham model

$$\frac{2U}{r_H} = \frac{r_H}{\mu}\left(-\frac{dP'}{dx}\right)\left[\frac{1}{a+b} - \frac{1}{b}\frac{T_1}{1-k} + \frac{a}{(a+b)b}\left(\frac{T_1}{1-k}\right)^{\frac{b}{a}+1}\right]$$

2. For the Ostwald-de Waele (Power-law) Model

$$\frac{2U}{r_H} = \frac{r_H}{K}\left(-\frac{dP'}{dx}\right)^{\frac{1}{n}}\left(\frac{n}{n+bn}\right)$$

3. For the Eyring model, no closed form can be obtained.

4. For the Ellis model

$$\frac{2U}{r_H} = \frac{\psi_0 r_H}{a+b}\left(-\frac{dP'}{dx}\right) + \frac{\psi_1}{b+ca}\left(-r_H\frac{dP'}{dx}\right)^a$$

5. For the Reiner-Philippoff model, no closed form can be obtained.

6. For the Rabinowitsch model

$$\frac{2U}{r_H} = \frac{1}{\mu_0}\left[\frac{r_H\left(-\frac{dP'}{dx}\right)}{a+b} + b_1\frac{r_H\left(-\frac{dP'}{dx}\right)^3}{3a+b}\right]$$

APPENDIX II GEOMETRIC CONSTANTS

Table 1 Geometric Constants for Annuli

k	a	b
0.00	0.25000	0.75000
0.01	0.37677	0.87509
0.03	0.40561	0.90854
0.05	0.42171	0.92626
0.07	0.43306	0.93828
0.10	0.44569	0.95095
0.20	0.46930	0.97370
0.30	0.48166	0.98472
0.40	0.48903	0.99109
0.50	0.49345	0.99466
0.60	0.49645	0.99728
0.70	0.49829	0.99882
0.80	0.49923	0.99944
0.90	0.49968	1.00000
1.00	0.50000	1.00000

APPENDIX II

Table 2 Geometric Constants for Rectangular Ducts

E	a	b
0.00	0.50000	1.00000
0.25	0.32124	0.81823
0.50	0.24398	0.72759
0.75	0.21779	0.68661
1.00	0.21206	0.67663

Table 3 Geometric Constants for Elliptical Ducts

β	a	b
0.00	0.30043	0.92528
0.10	0.30178	0.90534
0.20	0.29966	0.87199
0.30	0.27963	0.83080
0.40	0.27022	0.81066
0.50	0.26206	0.78859
0.60	0.25748	0.77245
0.70	0.25501	0.76849
0.80	0.25153	0.75450
0.90	0.25035	0.75103
1.00	0.25000	0.75000

APPENDIX II

Table 4 Geometric Constants for Isosceles Triangular Ducts

2ε	a	b
10°	0.15471	0.62780
20°	0.16930	0.63320
40°	0.18402	0.64223
60°	0.18753	0.64622
80°	0.18491	0.64384
90°	0.18302	0.63948

APPENDIX III DATA OF COMPARISON

Table 1 Values of Dimensionless Velocity $(2U/r_H)/(-r_H \frac{dP'}{dx}/K)^{\frac{1}{n}}$ for Power Law Fluid Flow in Annuli

n	Others[6]	Predicted k = 0.01	% Error[a]	Others[1]	Predicted k = 0.1	% Error
4	0.9350	1.0317	10.34	0.9060	0.9413	3.90
3	0.9169	0.9993	9.09	0.8791	0.9096	3.46
2	0.8017	0.9409	6.64	0.8305	0.8520	2.58
1	0.7908	0.7908	00.00	0.7161	0.7161	0.00
1/2	0.6859	0.6140	-10.50	0.5700	0.5429	-4.75
1/3	0.5915	0.4987	-15.70	0.4761	0.4372	-8.18
1/4	0.5161	0.4198	-18.66	0.4094	0.4109	-10.62
1/5	0.4562	0.3625	-20.55	0.3597	0.3146	-12.53
1/6	0.4092	0.3169	-21.68	0.3203	0.2759	-13.84
1/7	0.3691	0.2847	-22.87	0.2889	0.2457	-14.94
1/8	0.3357	0.2571	-23.64	0.2631	0.2215	-15.81
1/9	0.3095	0.2344	-24.25	0.2415	0.2016	-16.53
1/10	0.2852	0.2154	-24.75	0.2232	0.1850	-17.14

---

[6] Fredrickson and Bird, IEC, 50, No. 9, 347 (1958)

[a] 100 (Predicted - Others) / (Others)

APPENDIX III

Table 1 (Continued)

D	Others'	Predicted k = 0.2	% Error	Others'	Predicted k = 0.3	% Error
4	0.6901	0.9166	2.06	0.8942	0.9049	1.19
3	0.8609	0.8849	1.84	0.8640	0.8732	1.06
2	0.8163	0.8276	1.39	0.8095	0.8160	0.80
1	0.6990	0.6990	0.00	0.6819	0.6819	0.00
1/2	0.5971	0.5229	-2.64	0.5216	0.5139	-1.49
1/3	0.4400	0.4199	-4.74	0.4235	0.4116	-2.82
1/4	0.3742	0.3508	-6.72	0.3732	0.3495	-3.85
1/5	0.3256	0.2918	-7.59	0.3090	0.2947	-4.62
1/6	0.2883	0.2639	-0.47	0.2725	0.2581	-5.28
1/7	0.2588	0.2348	-9.26	0.2437	0.2295	-5.80
1/8	0.2347	0.2119	-9.70	0.2204	0.2067	-6.23
1/9	0.2140	0.1924	-10.03	0.2013	0.1880	-6.60
1/10	0.1931	0.1765	-10.90	0.1852	0.1724	-6.92

APPENDIX III

Table 1 (Continued)

n	Others'	Predicted k = 0.4	% Error	Others'	Predicted k = 0.5	% Error
4	0.8919	0.8982	0.70	0.8908	0.8945	0.40
3	0.8611	0.8665	0.63	0.8595	0.8627	0.37
2	0.8355	0.8393	0.45	0.8033	0.8056	0.28
1	0.6756	0.6756	0.00	0.6720	0.6720	0.00
1/2	0.5120	0.5070	-0.97	0.5074	0.5074	-0.54
1/3	0.4141	0.4068	-1.75	0.4081	0.4040	-0.98
1/4	0.3475	0.3393	-2.35	0.3416	0.3369	-3.09
1/5	0.2997	0.2910	-2.89	0.2938	0.2889	-1.67
1/6	0.2633	0.2540	-3.54	0.2577	0.2528	-1.91
1/7	0.2350	0.2265	-3.58	0.2297	0.2248	-2.13
1/8	0.2119	0.2039	-3.77	0.2069	0.2023	-2.22
1/9	0.1934	0.1854	-4.11	0.1884	0.1840	-2.33
1/10	0.1777	0.1700	-4.30	0.1728	0.1687	-2.42

APPENDIX III

Table 1 (Continued)

D	Others'	Predicted k = 0.6	% Error	Others'	Predicted k = 0.7	% Error
4	0.8899	0.8918	0.22	0.8893	0.8902	0.11
3	0.8599	0.8601	0.20	0.8577	0.8585	0.09
2	0.8010	0.8020	0.03	0.8008	0.8014	0.07
1	0.6695	0.6695	0.00	0.6680	0.6680	0.00
1/2	0.5040	0.5025	-0.30	0.5019	0.5012	-0.15
1/3	0.4030	0.4022	-0.47	0.4022	0.4010	-0.28
1/4	0.3378	0.3352	-0.76	0.3353	0.3342	-0.33
1/5	0.2903	0.2874	-0.99	0.2880	0.2865	-0.51
1/6	0.2545	0.2515	-1.17	0.2529	0.2507	-0.61
1/7	0.2267	0.2236	-1.36	0.2244	0.2229	-0.70
1/8	0.2042	0.2013	-1.44	0.2022	0.2006	-0.80
1/9	0.1858	0.1830	-1.53	0.1840	0.1824	-0.89
1/10	0.1705	0.1677	-1.62	0.1698	0.1672	-0.99

APPENDIX III

Table I (Continued)

n	Others'	Predicted k = 0.8	% Error	Others'	Predicted k = 0.9	% Error
4	0.8888	0.8895	0.05	0.8889	0.8890	0.00
3	0.8574	0.8577	0.04	0.8572	0.8572	0.00
2	0.8004	0.8006	0.03	0.8001	0.8001	0.00
1	0.6673	0.6673	0.00	0.6668	0.6660	0.00
1/2	0.5008	0.5005	-0.06	0.5002	0.5002	-0.01
1/3	0.4009	0.4006	-0.13	0.4003	0.4002	-0.02
1/4	0.3343	0.3337	-0.18	0.3338	0.3335	-0.09
1/5	0.2867	0.2861	-0.23	0.2860	0.2858	-0.06
1/6	0.2510	0.2503	-0.27	0.2503	0.2501	-0.06
1/7	0.2232	0.2223	-0.44	0.2225	0.2229	-0.09
1/8	0.2010	0.2003	-0.36	0.2003	0.2001	-0.11
1/9	0.1828	0.1821	-0.42	0.1821	0.1819	-0.13
1/10	0.1677	0.1669	-0.46	0.1670	0.1668	-0.15

APPENDIX III

Table 2 Values of Dimensionless Pressure Drop $\left(\frac{-r_H \frac{dP'}{dx}}{K}\right) / \left(\frac{2U}{r_H}\right)^n$ for Power Law Flow in Annuli

n	Others[o]	Predicted k = 0.01	% Error	Others'	Predicted k = 0.1	% Error
4	336.750	225.965	-32.90	383.210	326.032	-14.92
3	35.146	27.055	-23.10	39.734	35.880	-9.70
2	5.147	4.524	-12.10	5.798	5.510	-4.97
1	1.291	1.292	0.00	1.396	1.396	0.00
1/2	0.853	0.913	7.00	0.927	0.950	2.47
1/3	0.826	0.874	5.86	0.896	0.915	2.16
1/4	0.820	0.878	5.29	0.884	0.909	2.84
1/5	0.844	0.888	5.17	0.889	0.913	2.71
1/6	0.850	0.894	4.20	0.894	0.919	2.82
1/7	0.873	0.906	3.78	0.904	0.926	2.41
1/8	0.884	0.914	3.43	0.911	0.931	2.18
1/9	0.893	0.921	3.13	0.917	0.936	2.03
1/10	0.901	0.927	2.89	0.926	0.940	1.59

o Ref. 9

APPENDIX III

Table 2 (Continued)

n	Others'	Predicted	% Error	Others'	Predicted	% Error
		h = 0.2			h = 0.3	
4	393.630	362.730	-7.85	400.440	381.861	-4.64
3	41.166	39.972	-2.90	41.868	40.562	-3.12
2	6.003	5.840	-2.71	6.104	6.008	-1.58
1	1.443	1.443	0.00	1.466	1.466	0.00
1/2	0.965	0.970	1.04	0.980	0.987	0.75
1/3	0.911	0.926	1.63	0.923	0.932	0.96
1/4	0.905	0.919	1.63	0.915	0.924	0.98
1/5	0.900	0.922	1.57	0.917	0.926	0.93
1/6	0.914	0.926	1.40	0.921	0.930	0.91
1/7	0.919	0.932	1.14	0.927	0.935	0.86
1/8	0.924	0.936	1.31	0.932	0.939	0.81
1/9	0.894	0.941	1.23	0.936	0.943	0.76
1/10	0.984	0.945	1.16	0.940	0.947	0.72

APPENDIX III

Table 2 (Continued)

n	Others'	Predicted k = 0.4	% Error	Others'	Predicted k = 0.5	% Error
4	404.462	393.340	-2.75	406.590	399.959	-1.63
3	42.291	41.595	-1.86	42.521	42.049	-1.11
2	6.223	6.107	-0.95	6.233	6.164	-0.60
1	1.400	1.400	0.00	1.488	1.488	0.00
1/2	0.980	0.992	0.49	0.969	0.995	0.27
1/3	0.930	0.936	0.59	0.935	0.938	0.33
1/4	0.921	0.927	0.59	0.925	0.928	0.34
1/5	0.922	0.928	0.58	0.926	0.929	0.33
1/6	0.927	0.932	0.55	0.911	0.933	0.24
1/7	0.932	0.936	0.52	0.934	0.937	0.31
1/8	0.936	0.941	0.48	0.939	0.942	0.28
1/9	0.940	0.945	0.47	0.943	0.946	0.29
1/10	0.944	0.948	0.44	0.947	0.950	0.24

APPENDIX III

Table 2 (Continued)

D	Others'	Predicted k = 0.6	% Error	Others'	Predicted k = 0.7	% Error
4	408.360	404.719	-0.89	408.880	407.572	-0.32
3	42.697	42.437	-0.61	42.791	42.671	-0.28
2	6.256	6.218	-0.60	6.245	6.229	-0.13
1	1.494	1.494	0.00	1.497	1.497	0.00
1/2	0.996	0.998	0.15	0.998	0.999	0.08
1/3	0.928	0.940	0.16	0.940	0.940	0.07
1/4	0.920	0.929	0.17	0.929	0.930	0.08
1/5	0.928	0.930	0.20	0.930	0.931	0.10
1/6	0.932	0.934	0.19	0.933	0.934	0.10
1/7	0.936	0.938	0.18	0.938	0.939	0.10
1/8	0.940	0.942	0.18	0.941	0.942	0.10
1/9	0.945	0.946	0.17	0.946	0.946	0.10
1/10	0.948	0.950	0.16	0.950	0.950	0.10

APPENDIX III

Table 2 (Continued)

D	Others'	Predicted k = 0.8	% Error	Others'	Predicted k = 0.9	% Error
4	409.700	409.961	-0.10	410.070	409.946	-0.03
3	42.026	42.785	-0.12	42.859	42.863	0.01
2	6.247	6.241	-0.06	6.247	6.248	0.00
1	1.499	1.499	0.00	1.500	1.500	0.00
1/2	1.000	1.000	0.03	1.000	1.000	0.00
1/3	0.940	0.940	0.04	0.940	0.940	0.01
1/4	0.930	0.930	0.04	0.929	0.930	0.17
1/5	0.931	0.931	0.05	0.931	0.931	0.01
1/6	0.934	0.934	0.04	0.935	0.935	0.01
1/7	0.938	0.939	0.05	0.939	0.939	0.01
1/8	0.942	0.943	0.05	0.943	0.943	0.01
1/9	0.946	0.947	0.05	0.947	0.947	0.01
1/10	0.950	0.950	0.05	0.950	0.950	0.01

APPENDIX III

Table 3 Values of u_{max}/U for Power Law Flow in Annuli

n	Others'	Predicted k = 0.01	% Error	Others'	Predicted k = 0.1	% Error
∞	2.000	2.323	16.13	2.000	2.135	6.73
4	1.069	2.050	10.12	1.803	1.908	5.81
3	1.835	1.992	8.55	1.787	1.851	3.58
2	1.778	1.882	5.83	1.714	1.756	2.47
1	1.662	1.661	0.00	1.567	1.567	0.00
1/2	1.540	1.441	-6.46	1.419	1.378	-2.87
1/3	1.442	1.331	-7.72	1.342	1.284	-4.35
1/4	1.365	1.265	-7.36	1.280	1.227	-4.15
1/5	1.310	1.220	-6.84	1.240	1.189	-4.10
1/6	1.270	1.189	-6.38	1.210	1.162	-3.96
1/7	1.239	1.166	-5.95	1.187	1.142	-3.86
1/8	1.215	1.147	-5.60	1.168	1.126	-3.59
1/9	1.192	1.132	-5.01	1.154	1.113	-3.51
1/10	1.176	1.120	-4.74	1.140	1.103	-3.23
0	1.000	1.000	0.00	1.000	1.000	0.00

APPENDIX III

Table 3 (Continued)

n	Others'	Predicted k = 0.2	% Error	Others'	Predicted k = 0.3	% Error
∞	2.000	2.075	3.70	2.000	2.044	2.21
4	1.815	1.860	2.47	1.810	1.835	1.40
3	1.769	1.806	2.10	1.762	1.783	1.20
2	1.699	1.717	1.39	1.682	1.696	0.84
1	1.530	1.537	0.00	1.523	1.522	0.00
1/2	1.389	1.358	-1.57	1.361	1.348	-0.95
1/3	1.297	1.269	-2.18	1.278	1.261	-0.48
1/4	1.246	1.215	-2.49	1.227	1.209	-1.48
1/5	1.210	1.179	-2.55	1.194	1.174	-1.67
1/6	1.183	1.154	-2.49	1.168	1.149	-1.61
1/7	1.162	1.134	-2.38	1.146	1.131	-1.35
1/8	1.145	1.119	-2.23	1.130	1.116	-1.24
1/9	1.132	1.107	-2.17	1.117	1.104	-0.56
1/10	1.122	1.090	-1.99	1.106	1.095	-1.00
0	1.000	1.000	0.00	1.000	1.000	0.00

APPENDIX III

Table 9 (Continued)

n	Others'	Predicted k = 0.4	% Error	Others'	Predicted k = 0.5	% Error
∞	2.000	2.207	1.39	2.000	2.016	0.78
4	1.806	1.821	0.85	1.803	1.813	0.52
3	1.757	1.770	0.74	1.754	1.762	0.44
2	1.676	1.684	0.50	1.672	1.677	0.31
1	1.514	1.513	0.00	1.508	1.508	0.00
1/2	1.350	1.342	-0.58	1.344	1.339	-0.40
1/3	1.267	1.256	-0.82	1.261	1.254	-0.56
1/4	1.217	1.205	-0.96	1.212	1.203	-0.73
1/5	1.186	1.171	-1.26	1.180	1.169	-0.91
1/6	1.162	1.147	-0.46	1.146	1.145	-0.08
1/7	1.129	1.128	-0.06	1.127	1.127	0.00
1/8	1.114	1.114	-0.01	1.113	1.113	0.01
1/9	1.102	1.103	0.06	1.101	1.102	0.05
1/10	1.093	1.093	0.03	1.092	1.092	0.03
0	1.000	1.000	0.00	1.000	1.000	0.00

APPENDIX III

Table 3 (Continued)

D	Others'	Predicted k = 0.8	% Error	Others'	Predicted k = 0.9	% Error
∞	2.000	2.002	0.10	2.000	2.001	0.06
4	1.800	1.802	0.09	1.800	1.801	0.06
3	1.751	1.751	0.03	1.750	1.751	0.05
2	1.668	1.668	0.00	1.667	1.668	0.03
1	1.502	1.502	0.00	1.501	1.501	0.00
1/2	1.336	1.334	-0.15	1.334	1.334	-0.02
1/3	1.252	1.250	-0.12	1.251	1.250	-0.05
1/4	1.203	1.200	-0.22	1.201	1.200	-0.06
1/5	1.171	1.167	-0.34	1.169	1.167	-0.18
1/6	1.143	1.143	0.01	1.143	1.143	0.00
1/7	1.125	1.125	0.02	1.125	1.125	0.01
1/8	1.111	1.111	0.03	1.111	1.111	0.02
1/9	1.100	1.100	0.02	1.100	1.100	0.01
1/10	1.091	1.091	0.01	1.091	1.091	0.00
0	1.000	1.000	0.00	1.000	1.000	0.00

APPENDIX III

Table 6A Values of Dimensionless Velocity $\left(\frac{2U}{r_H}\right)/\left(\frac{-r_H \frac{dP'}{dx}}{\beta}\right)$ for Bingham Flow in Annuli

r_1	Others'	Predicted k = 0.01	% Error	Others'	Predicted k = 0.03	% Error
0.01	0.7873	0.7873	-0.06	0.7500	0.7496	-0.05
0.10	0.6833	0.6836	-0.68	0.6513	0.6477	-0.57
0.20	0.5793	0.5696	-1.67	0.5435	0.5340	-1.74
0.30	0.4731	0.4590	-2.98	0.4389	0.4281	-2.47
0.40	0.3712	0.3539	-4.66	0.3396	0.3264	-3.87
0.50	0.2755	0.2572	-6.65	0.2472	0.2333	-5.62
0.60	0.1803	0.1713	-9.01	0.1645	0.1518	-10.33
0.70	0.1126	0.0994	-11.70	0.0942	0.0845	-10.01
0.80	0.0624	0.0445	-15.09	0.0403	0.0352	-12.47
0.90	0.0120	0.0104	-10.63	0.0074	0.0062	-16.17

---

o Ref. 9

APPENDIX III

Table 4A (Continued)

F_1	Others'	Predicted k = 0.05	% Error	Others'	Predicted k = 0.07	% Error
0.01	0.7900	0.7905	-0.05	0.7181	0.7178	-0.04
0.10	0.6315	0.6285	-0.48	0.6175	0.6149	-0.43
0.20	0.5231	0.5169	-1.19	0.5079	0.5006	-1.43
0.30	0.4104	0.4092	-2.21	0.4025	0.3948	-1.92
0.40	0.3195	0.3006	-3.41	0.3034	0.2939	-3.13
0.50	0.2205	0.2169	-5.09	0.2130	0.2033	-4.53
0.60	0.1470	0.1377	-6.88	0.1340	0.1254	-6.38
0.70	0.0809	0.0736	-9.03	0.0697	0.0636	-8.63
0.80	0.0313	0.0277	-11.52	0.0239	0.0213	-10.53
0.90	0.0090	0.0032	-14.45	0.0014	0.0012	-13.44

APPENDIX III

Table 4 A (Continued)

T_1	Others'	Predicted k = 0.1	% Error	Others'	Predicted k = 0.2	% Error
0.01	0.7046	0.7044	-0.03	0.6803	0.6802	-0.02
0.10	0.6017	0.5996	-0.35	0.5664	0.5652	-0.21
0.20	0.4690	0.4655	-0.89	0.4437	0.4403	-0.76
0.30	0.3827	0.3763	-1.66	0.3279	0.3242	-1.13
0.40	0.2827	0.2752	-2.67	0.2234	0.2192	-1.85
0.50	0.1927	0.1849	-4.05	0.1337	0.1299	-2.78
0.60	0.11556	0.10932	-5.41	0.0632	0.0607	-3.93
0.70	0.05305	0.05115	-6.79	0.0168	0.0159	-5.51
0.80	0.01464	0.01328	-9.33	0.0000	0.0000	0.00
0.90	0.00000	0.00000	0.00			

APPENDIX III

Table 4 A (Continued)

T_1	Others'	Predicted k = 0.3	% Error	Others'	Predicted k = 0.4	% Error
0.01	0.66740	0.66791	0.06	0.65898	0.65891	-0.01
0.10	0.52046	0.51781	-0.12	0.50959	0.50899	-0.12
0.20	0.40099	0.39914	-0.24	0.35284	0.35139	-0.41
0.30	0.27450	0.27212	-0.51	0.21362	0.21207	-0.73
0.40	0.16490	0.16224	-1.61	0.10203	0.10068	-1.32
0.50	0.07018	0.07639	-2.29	0.02736	0.02689	-1.72
0.60	0.02079	0.02021	-2.00	0.00000	0.00000	0.00
0.70	0.00000	0.00000	0.00			

APPENDIX III

Table 4A (Continued)

T_1	Others'	Predicted	% Error	Others'	Predicted	% Error
		k = 0.5			k = 0.6	
0.01	0.65161	0.65101	-0.03	0.64445	0.64447	0.00
0.10	0.47326	0.47340	-0.18	0.42871	0.42401	-1.10
0.20	0.29192	0.29076	-0.40	0.21006	0.20948	-0.28
0.30	0.14121	0.14002	-0.84	0.05790	0.05773	-0.29
0.40	0.03927	0.03866	-1.04	0.00000	0.00000	0.00
0.50	0.00000	0.00000	0.00			
		k = 0.7			k = 0.8	
0.01	0.62477	0.62471	-0.01	0.61866	0.61719	-0.25
0.10	0.34796	0.34669	-0.39	0.21043	0.20842	-0.96
0.20	0.09972	0.09915	-0.57	0.00000	0.00000	0.00
0.30	0.00000	0.00000	0.00			
		k = 0.9				
0.01	0.56972	0.56712	0.25			
0.10	0.00000	0.00000	0.00			

APPENDIX III

Table 4B Values of $\left(\frac{2U}{V_N}\right)\rho/(1-k)\,T_y$ for Bingham Flow in Annuli

T_1	Others°	Author's $k = 0.01$	% Error°°	Others'	Author's $k = 0.03$	% Error°°
0.01	70.7796	70.7927		74.9951	74.9602	
0.10	6.0826	6.0958		6.5135	6.4769	
0.20	2.8964	2.8402		2.7174	2.6700	
0.30	1.5769	1.5299		1.4630	1.4269	
0.40	0.9201	0.8948		0.8489	0.8160	
0.50	0.5510	0.5144		0.4944	0.4666	
0.60	0.31377	0.28959		0.27410	0.25296	
0.70	0.16079	0.11369		0.13463	0.09657	
0.80	0.06947	0.05559		0.05932	0.04464	
0.90	0.01419	0.01155		0.00820	0.00668	

° Ref. 9

°° Same as in Table 4A

APPENDIX III

Table 4B (Continued)

T_1	Others'	Predicted $k = 0.1$	% Error*	Others'	Predicted $k = 0.2$	% Error*
0.01	70.4620	70.4625		68.0274	68.0161	
0.10	6.0169	5.9961		5.6636	5.6519	
0.20	2.4692	2.4274		2.2183	2.2014	
0.30	1.2757	1.2545		1.0931	1.0807	
0.40	0.7060	0.6879		0.5984	0.5801	
0.50	0.3854	0.3698		0.2673	0.2599	
0.60	0.19860	0.18220		0.10529	0.10115	
0.70	0.07035	0.05846		0.02404	0.01817	
0.80	0.01090	0.01659		0.00000	0.00000	
0.90	0.00000	0.00000				

* same as in Table 4A

APPENDIX III

Table 4 B (Continued)

T_1	Others'	Predicted k = 0.3	% Error	Others'	Predicted k = 0.4	% Error
0.01	66.7694	66.7905		65.8979	65.8909	
0.10	5.3946	5.3781		5.0959	5.0899	
0.20	2.0039	1.9957		1.7648	1.7570	
0.30	0.9150	0.9071		0.7121	0.7069	
0.40	0.4123	0.4056		0.2550	0.2517	
0.50	0.1564	0.1528		0.0547	0.0538	
0.60	0.03466	0.03368		0.0000	0.0000	
0.70	0.00000	0.00000				

APPENDIX III

Table 4B (Continued)

	Others'	Predicted	% Error*
T_I		k = 0.5	
0.01	65.1610	65.1010	
0.10	4.7426	4.7960	
0.20	1.4596	1.4938	
0.30	0.4707	0.4667	
0.40	0.0957	0.0967	
0.50	0.0000	0.0000	
T_I		k = 0.7	
0.01	63.4769	63.4712	
0.10	3.4796	3.4860	
0.20	0.4986	0.4957	
0.30	0.0000		
T_I		k = 0.9	
0.01	56.9715	56.7123	
0.10	0.0000	0.0000	

Others'	Predicted	% Error*
	k = 0.6	
64.4449	64.4474	
4.2071	4.2401	
1.0503	1.0474	
0.1930	0.1924	
0.0000		
	k = 0.8	
61.0659	61.7132	
2.1043	2.0842	
0.0000	0.0000	

* Same as in Table 4A

APPENDIX III

Table 3 Values of Dimensionless Pressure Drop $\left(\frac{-r_H \frac{dP'}{dx}}{\beta}\right) / \left(\frac{2U}{r_H}\right)$ for Bingham Flow in Annuli

r_1	Others'[a]	Predicted k = 0.01	% Error	Others'	Predicted k = 0.03	% Error
0.01	1.2694	1.2701	0.06	1.3334	1.3340	0.05
0.10	1.4629	1.4689	0.68	1.5353	1.5439	0.56
0.20	1.7269	1.7550	1.69	1.8400	1.8727	1.78
0.30	2.1139	2.1708	3.07	2.2784	2.3261	2.53
0.40	2.6930	2.8256	4.69	2.9450	3.0696	4.03
0.50	3.6296	3.8900	7.18	4.0450	4.2850	5.96
0.60	5.3117	5.8376	9.90	6.0809	6.5887	8.96
0.70	8.8049	10.0616	13.24	10.6113	11.8339	11.52
0.80	19.0924	22.4950	17.68	24.8429	28.3817	14.24
0.90	78.2779	96.2901	22.90	135.4646	161.6931	19.30

[a] Ref. 9

APPENDIX III

Table 5 (Continued)

T_1	Others'	Predicted k = 0.05	% Error	Others'	Predicted k = 0.07	% Error
0.01	1.3609	1.3609	0.00	1.3926	1.3932	0.04
0.10	1.5035	1.5918	0.48	1.6193	1.6263	0.43
0.20	1.9110	1.9367	1.20	1.9690	1.9976	1.45
0.30	2.3690	2.4490	2.26	2.4846	2.5331	1.95
0.40	3.1202	3.2408	3.03	3.2963	3.4029	3.23
0.50	4.3675	4.6110	5.26	4.6954	4.9180	4.74
0.60	6.7697	7.2631	7.30	7.4645	7.9732	6.81
0.70	12.3593	13.5515	9.92	14.3563	15.7117	9.44
0.80	31.9234	36.0315	13.09	41.9217	46.8582	11.78
0.90	266.1698	311.1300	16.89	730.4602	843.8819	15.53

APPENDIX III

Table 5 (Continued)

T_n	Others'	Predicted	% Error
		k = 0.1	
0.01	1.4892	1.4196	0.03
0.10	1.6620	1.6578	0.95
0.20	2.0415	2.0598	0.90
0.30	2.6130	2.6571	1.69
0.40	3.5259	3.6941	2.75
0.50	5.1079	5.4003	4.82
0.60	8.0537	9.1479	9.70
0.70	10.2239	19.8488	7.22
0.80	60.3013	75.3296	10.29
		k = 0.3	
0.01	1.4932	1.4972	-0.06
0.10	1.6571	1.6594	0.12
0.20	2.4990	2.5054	0.46
0.30	3.6439	3.6749	0.83
0.40	6.0642	6.1686	1.64
0.50	12.7982	13.0911	2.34
0.60	40.0990	49.4709	2.88

Others'	Predicted	% Error
	k = 0.2	
1.4700	1.4702	0.02
1.7657	1.7694	0.21
2.2540	2.2712	0.77
3.0495	3.0844	1.14
4.4768	4.5611	1.88
7.4816	7.6959	2.86
15.0285	16.4764	4.09
59.4283	62.8970	5.84
	k = 0.4	
1.5175	1.5177	0.01
1.9624	1.9647	0.12
2.8341	2.8458	0.41
4.7250	4.7155	-0.20
9.8023	9.9940	1.33
36.5524	37.1927	1.75

APPENDIX III

Table 5 (Continued)

T_1	Others'	Predicted	% Error
		k = 0.5	
0.01	1.5337	1.5242	-0.09
0.10	2.1005	2.1124	0.10
0.20	3.4256	3.4393	0.40
0.30	7.0019	7.1418	0.05
0.40	26.1322	25.0639	-1.09
		k = 0.7	
0.01	1.5764	1.5755	0.01
0.10	2.0739	2.0991	0.39
0.20	10.0202	10.0358	0.57
		k = 0.9	
0.01	1.7677	1.7633	-0.25

Others'	Predicted	% Error
	k = 0.6	
1.5517	1.5517	0.00
2.3326	2.3585	1.11
4.7606	4.7738	0.28
17.2712	17.3211	0.28
	k = 0.8	
1.6164	1.6204	0.25
4.7523	4.7981	0.96

APPENDIX III

Table 5 Values of u_{max}/U for Bingham Flow in Annuli

F_1	Others[a]	Predicted k = 0.01	% Error	Others'	Predicted k = 0.03	% Error
0.01	1.6565	1.6516	-0.30	1.6129	1.6107	-0.13
0.10	1.5094	1.5608	-1.54	1.5501	1.5310	-1.23
0.20	1.5294	1.4934	-2.76	1.4931	1.4946	-1.92
0.30	1.4573	1.4044	-3.69	1.4170	1.3739	-3.04
0.40	1.3836	1.3317	-3.73	1.3522	1.3041	-3.56
0.50	1.3296	1.2639	-4.90	1.2873	1.2404	-3.63
0.60	1.2522	1.2169	-2.82	1.2297	1.1817	-3.63
0.70	1.1855	1.1528	-2.76	1.1694	1.1302	-2.05
0.80	1.1198	1.0990	-1.86	1.1005	1.0746	-2.35
0.90	1.0562	1.0549	-0.22	1.0407	1.0375	-0.31

[a] Ref. 9

APPENDIX III

Table 6 (Continued)

T_1	Others'	Predicted k = 0.05	% Error	Others'	Predicted k = 0.07	% Error
0.01	1.5099	1.5091	-0.11	1.5757	1.5742	-0.10
0.10	1.5255	1.5103	-1.06	1.5098	1.4956	-0.94
0.20	1.4502	1.4297	-1.96	1.4406	1.4210	-1.36
0.30	1.3923	1.3564	-2.61	1.3743	1.3421	-2.34
0.40	1.3207	1.2879	-3.08	1.3104	1.2760	-2.63
0.50	1.2653	1.2267	-3.05	1.2484	1.2139	-2.76
0.60	1.2045	1.1609	-2.95	1.1879	1.1591	-2.43
0.70	1.1490	1.1156	-1.66	1.1294	1.1095	-1.76
0.80	1.0851	1.0666	-0.06	1.0336	1.0571	2.28
0.90	1.0265	1.0218	-0.46	1.0059	1.0143	0.84

APPENDIX III

Table 6 (Continued)

T_1	Others'	Predicted	% Error
		k = 0.1	
0.01	1.5504	1.5501	-0.09
0.10	1.4919	1.4790	-0.08
0.20	1.4205	1.3905	-1.54
0.30	1.3535	1.3254	-2.08
0.40	1.2875	1.2589	-2.23
0.50	1.2270	1.1990	-2.28
0.60	1.1670	1.1407	-2.25
0.70	1.1099	1.0835	-2.23
0.80	1.0591	1.0497	-0.89
		k = 0.3	
0.01	1.5817	1.5800	-0.12
0.10	1.4260	1.4160	-0.42
0.20	1.2953	1.2860	-0.63
0.30	1.2350	1.2455	-0.89
0.40	1.1851	1.1751	-0.85
0.50	1.1462	1.1093	-0.62
0.60	1.0945	1.0801	-0.60

Others'	Predicted	% Error
	k = 0.2	
1.5283	1.5275	-0.06
1.4510	1.4432	-0.54
1.3725	1.3611	-0.82
1.2999	1.2837	-1.25
1.2329	1.2149	-1.46
1.1700	1.1529	-1.45
1.1099	1.0971	-1.15
1.0547	1.0470	-0.73
	k = 0.4	
1.5009	1.5009	-0.03
1.3983	1.3950	-0.29
1.2989	1.2933	-0.39
1.2119	1.2054	-0.54
1.1338	1.1285	-0.47
1.0718	1.0564	-0.14

APPENDIX III

Table 6 (Continued)

T_R	Others'	Predicted	% Error	Others'	Predicted	% Error
		k = 0.5			k = 0.6	
0.01	1.4926	1.4928	-0.05	1.4660	1.4654	-0.04
0.10	1.3716	1.3697	-0.14	1.3374	1.3360	-0.11
0.20	1.2503	1.2464	-0.15	1.2092	1.2019	-0.11
0.30	1.1291	1.1277	-0.22	1.1092	1.0902	-0.12
0.40	1.0751	1.0402	-0.25			
		k = 0.7			k = 0.8	
0.01	1.4774	1.4779	-0.01	1.4614	1.4648	0.23
0.10	1.3563	1.3567	0.03	1.3076	1.3015	-0.51
0.20	1.1294	1.1245	-0.43			
		k = 0.9				
0.01	1.4927	1.4891	-0.25			

APPENDIX III

Table 7 Values of Dimensionless Velocity $\left(\frac{2U}{r_H}\right)/\left(\frac{-r_H \frac{dP'}{dx}}{\rho_o}\right)$ for Rabinowitsch Flow in Annuli

k	C_1	Rotem's[o]	Predicted	% Error
0.1	0	0.7161	0.7161	0.00
0.1	5	2.6041	2.4417	-9.03
0.1	10	4.6123	4.1672	-9.65
0.1	20	8.4682	7.6183	-10.04
0.1	30	12.3269	11.0695	-10.20
0.2	0	0.6930	0.6930	0.00
0.2	5	2.1262	2.0366	-4.12
0.2	10	3.5342	3.3803	-4.36
0.2	20	6.3551	6.0675	-4.53
0.2	30	9.0282	8.7548	-3.03
0.5	0	0.6719	0.6719	0.00
0.5	5	1.1797	1.1770	-0.23
0.5	10	1.6963	1.6820	-0.84
0.5	20	2.7451	2.6921	-1.93
0.5	30	3.7375	3.7022	-0.94
0.9	0	0.6668	0.6668	0.00
0.9	5	0.6895	0.6868	-0.39
0.9	10	0.7074	0.7068	-0.08
0.9	20	0.7495	0.7468	-0.35
0.9	30	0.7904	0.7869	-0.45

o K. Rotem ASME Series E 84 421-424 (1962)

APPENDIX III

Table 9 Values of Dimensionless Velocity $(2U/r_H)/\left(\frac{-r_H}{K}\frac{dP'}{dx}\right)^{\frac{1}{n}}$ for Pseudoplastic Flow in Rectangular Ducts

E	B	Schechter's[o]	Wheeler and Wissler[o]	Predicted	% Error[ooo]
1	1	1.1282	1.1246	1.1252	0.36
1	3/4	1.0633	1.0680	1.0423	1.97
1	1/2	0.9662	0.9772	0.9085	5.98
3/4	1	1.1290	-	1.1057	1.18
3/4	3/4	1.0698	1.0699	1.0296	3.96
3/4	1/2	0.9764	-	0.8911	8.73
1/2	1	1.0569	1.0296	1.0293	2.50
1/2	3/4	0.6557[oooo]	0.9755	0.9525	43.10
1/2	1/2	0.8795	-	0.8227	6.46
1/4	1	0.8707	-	0.8776	0.79
1/4	3/4	0.8130	-	0.8022	1.33
1/4	1/2	0.7257	-	0.6846	5.66
0	1	0.6667	-	0.6667	0.00
0	3/4	0.6000	-	0.6000	0.00
0	1/2	0.5000	-	0.5000	0.00

o Ref. 10, oo Ref. 19, ooo Comparisons are made between Schechter's and the predicted values.
oooo This value has been found in error

APPENDIX III

Table 10 Values of Dimensionless Pressure Drop $\left(\frac{-g_H \frac{dP'}{dz}}{K}\right)/\left(\frac{2U}{r_H}\right)^{2-n}$ for Pseudoplastic Flow in Rectangular Ducts

B	A	Schechter's	Wheeler and Wheeler	Predicted	% Error*
1	1	0.6019	0.8892	0.6887	0.36
1	3/4	0.7699	0.7670	0.7810	1.52
1	1/2	0.7890	0.7152	0.7420	3.20
3/4	1	0.6937	-	0.9044	1.20
3/4	3/4	0.7680	0.7769	0.7920	3.23
3/4	1/2	0.7155	-	0.7490	4.68
1/2	1	0.9745	0.9715	0.9716	0.30
1/2	3/4	1.0518oo	0.8209	0.8883	16.32
1/2	1/2	0.7540	-	0.7790	3.32
1/3	1	1.1405	-	1.1395	0.79
1/4	3/4	0.9413	-	0.9501	0.93
1/4	1/2	0.8300	-	0.8546	2.96
0	1	1.5000	-	1.5000	0.00
0	3/4	1.1020	-	1.1020	0.00
0	1/2	1.0000	-	1.0000	0.00

o Comparisons are made between Schechter's and the predicted values

oo This value has been found to be in error

APPENDIX III

Table 11 Values of u_{max}/U for Pseudoplastic Flow in Rectangular Ducts

E	B	Schechter's	Predicted	% Error
1	1	2.1249	2.0954	-1.65
1	3/4	1.9905	1.9389	-2.57
1	1/2	1.7895	1.7301	-3.31
3/4	1	2.1237	2.0769	-2.39
3/4	3/4	1.9889	1.9226	-3.31
3/4	1/2	1.7972	1.7176	-4.43
1/2	1	2.0493	1.9910	-2.84
1/2	3/4	1.9445	1.8495	-4.88
1/2	1/2	1.7819	1.6607	-6.80
1/4	1	1.8676	1.7795	-5.04
1/4	3/4	1.8142	1.6630	-8.33
1/4	1/2	1.7211	1.5157	-11.93
0	1	1.5000	1.5000	0.00
0	3/4	1.4625	1.4206	-0.90
0	1/2	1.3618	1.3333	-0.60

APPENDIX III

Table 18 The Friction Factor - Reynolds Number Product for Pseudoplastic Flow Through Rectangular Ducts

B	D	Wheeler and Wheeler's[o]	Schechter's	Predicted	% Error[ooo]
1	1.00	56.91	57.08	56.90	0.00
1	0.90	47.62	-	47.87	0.53
1	0.80	39.66	-	40.50	1.30
1	0.75	36.22	36.24	36.89	1.04
1	0.70	33.07	-	33.51	1.33
1	0.60	27.59	-	28.30	2.79
1	0.50	22.69	23.02	23.74	3.67
1	0.40	18.97	-	19.85	4.66
0.75	0.75	48.05	47.51	48.97	1.93
0.50	1.00	139.90	140.40	139.91	0.00
0.50	0.75	70.83	105.00[oo]	80.62	2.02

[o] J.A. Wheeler and E.N. Wheeler, AIChE Journal, 11, 207 (1965)

[oo] This value has been found in error

[ooo] Wheeler and Wheeler's values are used for comparison

APPENDIX III

Table 13 Values of Dimensionless Velocity $(2U/r_H)/\left(\frac{-r_H \frac{dP'}{dx}}{K}\right)^{\frac{1}{n}}$ for Power Law Fluid Flow in Elliptical Ducts

β	n	Others'	Predicted	% Error
0.8	2.0	1.1326	1.1339	0.29
0.8	1.5	1.0827	1.0843	0.14
0.8	1.0	0.9939	0.9939	0.00
0.8	0.8	0.9359	0.9354	-0.05
0.8	0.6	0.8528	0.8519	0.10
0.8	0.4	0.7225	0.7220	0.05
0.6	2.0	1.1063	1.1096	0.30
0.6	1.5	1.0606	1.0592	-0.13
0.6	1.0	0.9709	0.9709	0.00
0.6	0.8	0.9153	0.9130	-0.16
0.6	0.6	0.8343	0.8322	-0.25
0.6	0.4	0.7074	0.7058	-0.17
0.4	2.0	1.0334	1.0574	2.32
0.4	1.5	0.9997	1.0093	0.96
0.4	1.0	0.9252	0.9252	0.00
0.4	0.8	0.8720	0.8708	-0.14
0.4	0.6	0.7927	0.7930	0.04
0.4	0.4	0.6669	0.6729	0.90

APPENDIX III

Table 14 Values of Dimensionless Pressure Drop $\left(\frac{-r_H \frac{dP'}{dz}}{K}\right)/\left(\frac{2U}{r_H}\right)^n$ for Power Law Flow in Elliptic Ducts

β	n	Others[9]	Author's	% Error
0.8	2.0	3.1182	3.0995	-0.60
0.8	1.5	1.6396	1.6385	0.48
0.8	1.0	1.0061	1.0061	0.00
0.8	0.8	0.8820	0.8824	0.04
0.8	0.6	0.8103	0.8103	0.00
0.8	0.4	0.7894	0.7892	0.02
0.6	2.0	3.2681	3.2486	-0.59
0.6	1.5	1.6818	1.6859	0.20
0.6	1.0	1.0299	1.0299	0.00
0.6	0.8	0.8979	0.8990	0.13
0.6	0.6	0.8205	0.8210	0.15
0.6	0.4	0.7961	0.7967	0.07
0.4	2.0	3.7457	3.5778	-4.48
0.4	1.5	1.8909	1.8118	-1.43
0.4	1.0	1.0309	1.0309	0.00
0.4	0.8	0.9334	0.9334	0.11
0.4	0.6	0.8461	0.8459	-0.02
0.4	0.4	0.8154	0.8122	-0.39

---

[9] Ref. 20

APPENDIX III

CORRECTION*

$\frac{h}{D}$	λ_ϕ (T_o = 0.01)		ϕ_o (T_o = 0.01)		B (T_o = 0.01)	
	Erroneous	Corrected	Erroneous	Corrected	Erroneous	Corrected
0.00	0.0000	0.0100	0.5000	0.49005	1.0000	0.98667
0.01	0.3295	0.3334	0.3252	0.31935	0.7770	0.77204
0.03	0.3776	0.3814	0.2902	0.28452	0.7101	0.70499
0.05	0.4080	0.4121	0.2675	0.26233	0.6644	0.65792
0.07	0.4326	0.4367	0.2497	0.24466	0.6249	0.61892
0.10	0.4637	0.4679	0.2279	0.22251	0.5726	0.56504
0.20	0.5461	0.5505	0.1671	0.16635	0.4271	0.41796
0.30	0.6147	0.6193	0.1271	0.12361	0.3059	0.29763
0.40	0.6770	0.6817	0.09204	0.08902	0.2097	0.19928
0.50	0.7355	0.7403	0.06330	0.06083	0.1325	0.12218
0.60	0.7915	0.7963	0.04044	0.03833	0.0754	0.06599
0.70	0.8455	0.8504	0.02214	0.02110	0.03728	0.02914
0.80	0.8981	0.9030	0.00990	0.00904	0.01496	0.00891
0.90	0.9495	0.9545	0.002480	0.002026	0.004334	0.001749
1.00	1.0000	1.0000	0.00000	0.00000	0.00000	0.00000

* The column for T_o = 0.01 in Table I, Ref. 9, has been found to be in error

APPENDIX IV DERIVATION OF EQUATIONS

A. The Rabinowitsch-Mooney Equations

1. Pipes

The volumetric flow rate for pipes is given by

$$Q = 2\pi \int_0^R u r \, dr$$

$$= -\pi \int_0^R r^2 \frac{du}{dr} \, dr \qquad \text{(AIV-1)}$$

From momentum considerations, one finds

$$r = \frac{R}{\tau_w} \tau \qquad \text{(AIV-2)}$$

Inserting r into Eq. (AIV-1), we obtain

$$Q = -\frac{\pi R^3}{\tau_w^3} \int_0^{\tau_w} \left(\frac{du}{dr}\right) \tau^2 \, d\tau$$

$$\frac{dQ}{d\tau_w} \frac{\tau_w^3}{} = -R^3 \left(-\frac{du}{dr}\right)_w \tau_w^2$$

$$\left(-\frac{du}{dr}\right)_w = \frac{\tau_o}{\pi R^3} \frac{dQ}{d\tau_w} + 3\frac{Q}{\pi R^3}$$

$$= \tau_w \frac{d\frac{U}{R}}{d\tau_w} + 3\frac{U}{R}$$

$$= \frac{1}{4} \tau_w \frac{d\left(\frac{8U}{D}\right)_w}{d\tau_w} + \frac{3}{4}\frac{8U}{D_H} \qquad \text{(AIV-3)}$$

APPENDIX IV

2. Parallel plates

The volumetric flow rate for parallel plates is

$$Q = 2\Delta Z \int_0^{y_o} u\,dy$$

$$= -2\Delta Z \int_0^{y_o} y \frac{du}{dy}\,dy \qquad \text{(AIV-4)}$$

From momentum considerations, one finds

$$y = \frac{y_o}{\tau_w}\,\tau \qquad \text{(AIV-5)}$$

Inserting y into Eq. (AIV-4), we get

$$Q = -2\Delta Z \frac{y_o^2}{\tau_w^2} \int_0^{\tau_w} \tau \frac{du}{dy}\,d\tau$$

$$\frac{dQ\,\tau_w^2}{d\tau_w} = 2(\Delta Z)\, y_o^2\, \tau_w \left(-\frac{du}{dy}\right)_w$$

$$\left(-\frac{du}{dy}\right)_w = \frac{\tau_w}{2(\Delta Z)\, y_o^2} \frac{dQ}{d\tau_w} + \frac{Q\,\tau_w}{(\Delta Z)\,\tau_w\, y_o^2}$$

$$= \frac{1}{2}\tau_w \frac{d\frac{2U}{y_o}}{d\tau_w} + \frac{2U}{y_o} \qquad \text{(AIV-6)}$$

$$= \frac{1}{2}\tau_w \frac{d\frac{2U}{\sigma_M}}{d\tau_w} + \frac{2U}{\sigma_M}$$

APPENDIX IV

B. The maximum velocity for Bingham flow through parallel plates

$$u_{max} = \frac{y_o}{\tau_w} \int_{\tau_y}^{\tau_w} f(\tau)\, d\tau$$

$$= \frac{y_o}{\tau_w} \int_{\tau_y}^{\tau_w} \frac{\tau - \tau_y}{\beta}\, d\tau$$

$$= \frac{y_o}{\beta \tau_w} \left[\frac{1}{2} \tau^2 - \tau_y \tau \right]_{\tau_y}^{\tau_w}$$

$$= \frac{y_o}{\beta \tau_w} \left[\frac{1}{2} (\tau_w^2 - \tau_y^2) - \tau_y (\tau_w - \tau_y) \right]$$

$$= \frac{\tau_w y_o}{2\beta} \left[1 + \left(\frac{\tau_y}{\tau_w}\right)^2 - 2\left(\frac{\tau_y}{\tau_w}\right) \right]$$

APPENDIX V INCLUSION OF THE EFFECTIVE SLIP VELOCITY IN THE GENERAL RABINOWITSCH-MOONEY EQUATION

The Rabinowitsch-Mooney equation applicable to circular ducts and parallel plates including slip velocity at the wall is

$$\left(-\frac{8}{n}\right) = f(\tau_w) = a\,\tau_w \frac{d\,\frac{2(U-v_w)}{r_H}}{d\,\tau_w} + b\,\frac{2(U-v_w)}{r_H}$$

v_w is the effective slip velocity at the wall presumed to be a function of τ_w. For flow through any shape cross-section, this equation is generalized as follows

$$\frac{1}{C}\oint_C f(\tau_w)\,dl = a\,\tau_0 \frac{d\,\frac{2(U-v_0)}{r_H}}{d\,\tau_0} + b\,\frac{2(U-v_0)}{r_H}$$

where $$v_0 = \frac{1}{C}\oint_C v_w\,dl$$

$$\tau_0 = \frac{1}{C}\oint_C \tau_w\,dl = r_H\left(-\frac{dP'}{dx}\right)$$

There is no data available concerning the relationship of v_0 and τ_0, and the obvious assumption in this instance is that the relationship is the same as between v_w and τ_w. The quantity $\frac{1}{C}\oint f(\tau_w)\,dl$ is equal to $f(\tau_w)$ in the case of flow through circular cross sections and between parallel plates, as well as for the flow of Newtonian, Bingham, etc. fluids

APPENDIX V

through any shape cross-section. For this reason, it is convenient to assume that

$$\frac{1}{C}\oint_C f(\tau_w)\,dl = f(\tau_g)$$

That gets around the difficulty of requiring a knowledge of the shear stress distribution along the contour corresponding to the wetted perimeter. Thus the generalised Rabinowitsch Mooney equation becomes

$$f(\tau_0) = a\tau_0 \frac{d\left(\frac{2(U-a_0)}{\tau_H}\right)}{d\tau_0} + b\,\frac{2(U-a_0)}{\tau_H}$$

APPENDIX VI HYDRAULIC RADII

Ducts	r_H
Circular tubes	$R/2$
Parallel plates	y_o
Annuli	$\frac{(1-k)\,r_o}{2}$
Rectangular ducts	$\frac{b'}{1+E}$
Elliptic ducts	$\frac{\pi\, b'}{4\, E_o}$
Isosceles triangular ducts	$\frac{a}{2}\ \frac{\sin\alpha}{1+\sin\alpha}$

APPENDIX VII SAMPLE CALCULATIONS

Four examples in Fredrickson and Bird's paper (9) are reworked.

Example 1. Calculation of Pressure Drop for Annular Flow of a Bingham Plastic Material.

Given: $U = 5 \frac{ft}{sec}$

$r_0 = 0.0065$ ft

$k = 0.496$

$r_M = \frac{(1 - k) r_0}{2}$

$\tau_y = 0.554 \frac{lb_f}{ft^2}$

$\rho = 0.000502\ lb_f\ (sec)/ft^2$

Solution: The quantity listed in Table 4B, Appendix IX, is

$$\frac{c_D}{\tau_1} = \frac{(\frac{2U}{r_M})\rho}{(1 - k)\tau_y} = \frac{4U\rho}{r_0 (1 - k)^2 \tau_y}$$

$$= \frac{20\ (0.000502)}{(0.0065)\ (0.504)^2\ (0.554)}$$

$$= 0.69$$

This value corresponds to a τ_e value of 0.298

APPENDIX VII

$$\frac{(c_B)_1}{(c_B)_2} = \frac{U_1 \left(-\frac{dP'}{dx}\right)_2}{U_2 \left(-\frac{dP'}{dx}\right)_1}$$

$$= \frac{(5)(28.3)}{(10)(16.8)} = 0.849$$

The definition of T_1 gives

$$\frac{(T_1)_1}{(T_1)_2} = \frac{\left(-\frac{dP'}{dx}\right)_2}{\left(-\frac{dP'}{dx}\right)_1} = 1.685$$

A trial-and-error method is used to calculate $(T_1)_1$. By assuming $(T_1)_1$, $(T_1)_2$ can be evaluated. Use these two T_1 and check the ratio $\frac{(c_B)_1}{(c_B)_2}$.

For $(T_1)_1 = 0.198$

$$\frac{(c_B)_1}{(c_B)_2} = \frac{(0.4482)}{(0.592)} = 0.842$$

$$p = \frac{r_H^2 \left(-\frac{dP'}{dx}\right)_1 (c_B)_1}{2U_1} = \frac{(1-k)^2 r_0^2 \left(-\frac{dP'}{dx}\right)_1 (c_B)_1}{8U_1}$$

$$= \frac{(0.592)^2 (0.00439)^2 (16.8)(0.4482)}{8(5)}$$

$$= 0.000497 \text{ lb}_f (\text{sec})/\text{ft}^2 \qquad (\Delta = 0)$$

APPENDIX VII

$$\left(-\frac{dP'}{dx}\right) = \frac{K(2U)^n}{(r_H)^{1+n}}\left(\frac{a+bn}{n}\right)^n$$

$$= \frac{(0.00495)(10)^{1.716}(1.1250)^{0.716}}{\left(\frac{(0.594)(0.0863)}{2}\right)(0.716)}$$

$$= 25.6 \ (lb_f/ft^3) \qquad \text{(Ans)}$$

Fredrickson and Bird obtained 25.6 $\frac{lb_f}{ft^3}$ for the pressure gradient.

Example 4. Deduction of Power Law Constants from Flow Through an Annulus

Given: $k = 0.496$

$r_o = 0.0863$ ft

Two sets of data are

$Q_1 = 0.09775 \ ft^3/sec$, $P_1 = 326 \ lb_f/ft^3$

$Q_2 = 0.19550 \ ft^3/sec$, $P_2 = 460 \ lb_f/ft^3$

or $U_1 = 5$ ft/sec, $U_2 = 10$ ft/sec

Solution: Use the following equation,

$$\frac{-r_H \frac{dP'}{dx}/k}{(2U/r_H)^n n^{-n}} = (a+bn)^n$$

APPENDIX VII

$$\frac{\left(-\frac{dP'}{dx}\right)_1}{\left(-\frac{dP'}{dx}\right)_2} = \left(\frac{U_1}{U_2}\right)^n$$

$$\frac{326}{460} = \left(\frac{0.09775}{0.19550}\right)^n$$

$$n = 0.5 \qquad \text{(Ans)}$$

$$K = \frac{r_H \left(-\frac{dP'}{dx}\right)_1 n^n}{(2U_1/r_H)^n (a + bn)^n}$$

$$K = \frac{r_H^{1+n} \left(-\frac{dP'}{dx}\right)_1 n^n}{(2U_1)^n (a + bn)^n}$$

$$= r_H^{1+n} \left(\frac{dP'}{dx_1}\right) \left(\frac{n}{2U_1 (a + bn)}\right)^n$$

$$= \left(\frac{(0.594)(0.000695)}{2}\right)^{1.5} (326) \left(\frac{0.5}{(10)(0.49 + 0.99 \times 0.5)}\right)^{0.5}$$

$$= (0.000415)(326)(0.225)$$

$$= 0.304 \text{ lb}_f \text{ (sec)}^{0.5}/\text{ft}^2 \qquad \text{(Ans)}$$

Prediction and Bird's solutions are: $K = 0.30 \frac{\text{lb}_f \text{ sec}^{0.5}}{\text{ft}^2}$ and $n = 0.5$.

NOMENCLATURE

a, b	=	geometric parameters, defined by Eq. (5-6)
a', b'	=	half lengths of major and minor side of rectangular ducts
a', b'	=	half lengths major and minor semi-axes of elliptic ducts
b_1	=	parameter in Rabinowitsch model
A	=	constant in Eq. (4-5), lb_f sec/sq ft
A, B	=	parameters in Eyring-Powar model. A has units of sec^{-1} and B has units of sq ft/lb_f
C	=	duct circumference, ft
C_1	=	$b_1 \left(\frac{P\, z_M}{1 - E}\right)^2$, dimensionless
D	=	diameter, ft
E	=	modulus of elasticity (Young's modulus), lb_f/sq ft
E	=	energy of activation, defined in Eq. (4-5)
E_0	=	elliptic integral of the second kind
f	=	Fanning friction factor, dimensionless
$f(\tau)$	=	$-\frac{du}{d\tau}$, sec^{-1}
G_c	=	dimensional conversion factor in Newton's second law, 32.2 lb_m ft/sec^2 lb_f
G	=	shearing modulus of elasticity, lb_f/sq ft
h	=	elevation, ft
k	=	ratio of radius of inner cylinder to that of outer cylinder, r_i/r_o, dimensionless

Q	=	volumetric flow rate, ft^3/sec
r	=	radius, ft
r_i	=	inner annulus half diameter
r_o	=	outer annulus half diameter
R	=	radius of pipe, ft
R	=	constant in the perfect gas law, 1545 ft lb_f/lb mole °R
s	=	effective slip velocity, ft/sec
t	=	time sec
T	=	temperature, °R
τ	=	shear stress lb_f/sq ft
τ_1	=	$\tau_y (1 - k)/P r_H$, dimensionless
τ_o	=	average shear stress at the wall, defined in Eq. (5-2)
τ_T	=	tensile stress, lb_f/sq ft
τ_w	=	shear stress at the wall, lb_f/sq ft
τ_y	=	limiting shear stress of Bingham plastics, lb_f/sq ft
τ_{ij}	=	stress acting on a plane perpendicular to the direction j, and acting in the direction i
u	=	local velocity, ft/sec
U	=	average velocity ft/sec
U_f	=	bulk velocity of fcc ft/sec
y_o	=	one half the distance between parallel plates, ft
Z	=	stability factor (29), dimensionless

α = kinetic energy correction factor α, dimensionless

θ = half opening of isosceles triangular ducts

α_B = function defined in Eq. (7-10)

β = constant in the Bingham plastic model

β = ratio of the minor semi-axis to the major

γ = $g_c K' \theta^{n'-1}$, $lb_m/sec^{2-n} ft$

γ = shearing strain, dimensionless

γ_T = fractional elongation or strain, dimensionless

ζ = a/T_w, effective slip velocity coefficient, $ft^3/lb\ sec$

η = apparent viscosity, $lb_f\ sec/sq\ ft$

μ_0 = parameter in the Rabinowitsch model

μ_0, μ_∞, T_0 = parameters in the Reiner-Philippoff model

μ_f = Newtonian viscosity, $lb_f\ sec/ft^2$

μ_m = Newtonian viscosity, $lb_m/sec\ ft$

π = 3.1415 ...

ρ = density, lb_m/ft^3

σ = specific weight, lb_f/ft^3

ϕ = $\dfrac{4}{T_w^4} \displaystyle\int_0^{T_w} T^2 f(T)\, dT$

ψ_0, ψ_1 = parameters in the Ellis model

16. T. S. Lundgren, E. M. Sparrow, J. B. Starr, ASME, Ser. D, 86, 623 (1964)

17. J. G. Knudsen, D. L. Katz, "Fluid Dynamics and Heat Transfer", McGraw-Hill, 104 - 104, (1958)

18. R. S. Schechter, A. I. Ch. E. Journal, 7, No. 3, 445 (1961)

19. J. A. Wheeler and E. H. Wissler, A. I. Ch. E. Journal, 11, No. 2, 207 (1965)

20. T. Miyauchi, N. Mitsuishi, and R. Nakamura, Chem. Eng., Japan, 28, 648 - 652 (Aug. 1964)

21. N. W. Ryan, W. E. Stevens, and E. B. Christiansen, A. I. Ch. E. Journal, 1, 544 (1955)

22. N. C. Claiborne, ORNL 1248, Oak Ridge National Laboratory, Oak Ridge, Tennessee (1952)

23. N. W. Ryan, M. M. Johnson, A. I. Ch. E. Journal, 5, 433 (1959)

24. R. W. Hanks, E. B. Christiansen, A. I. Ch. E. Journal, 8 467 (1962)

25. R. W. Hanks, A. I. Ch. E. Journal, 9, 45 (1963)

26. C. Mack, J. Polymer Sci., 19, 279 (1956)

27. M. Reiner, "Phenomenological Macrorheology" in "Rheology", Vol. 1, F. R. Eirich (Ed.), Academic Press, Inc., New York (1956)

28. V. L. Streeter, "Fluid Mechanics", P. 3, (1962)

29. A. B. Metzner, "Non-Newtonian Technology" in "Advances in Chemical Engineering", Vol. 1, T. B. Drew and J. W. Hoopes (Eds), Academic Press, Inc., New York (1956).

30. W. K. Lewis, L. Squires, and Broughton, "Industrial Chemistry of Colloidal and Amorphous Materials", MacMillan, New York (1942)

31. da C. Andrade, E.N., Endeavour, 13, 117 (1954)

32. W. Kozicki, unpublished work

33. W.L. McCabe and J.C. Smith, "Unit Operation of Chemical Engineering", McGraw-Hill (1956)

34. F.H. Caskins and W. Philippoff, Trans. Soc. Rheol. 3, 181 (1959)

35. Y.C. Yen and C. Tien, Can. J. Chem. Eng., 41, No. 2, 83 (1963)

36. W. Kozicki, and K.S. Yuan, Can. J. Chem. Eng., 41, 280 (1963)

37. A.B. Metzner, and J.C. Reed, A.I.Ch.E. Journal, 1, 434 (1955)

38. D.L. McIntosh, "Elastic Effects in the Extrusion of Polymer Solutions," doctoral thesis, Washington University, St. Louis (1960)

39. E.M. Sparrow, A.I.Ch.E. Journal, 8, No. 5, 599 (1962)

40. C. Tiu, M.Sc. thesis, University of Ottawa (1969)

41. E.B. Bagley, J. Appl. Phys., 28, 624 (1957)

42. J.M. McKelvey, "Polymer Processing", Wiley, N.Y. (1962)

43. E.B. Christiansen, N.W. Ryan, and W.E. Stevens, A.I.Ch.E. Journal, 1, No. 4, 545 (1955)

44. A. Pontius and J.S. Slick, D.Ch.E. thesis, University of Delaware, Newark (1954)

45. G.W. Govier, and M.D. Wiming, Ind. Eng. Chem., 44, 651 (1952)

46. M. Collins and W.R. Schowalter, A.I.Ch.E. Journal, 9, 804 (1963)

47. M. Reiner, J. Rheol. 1, 250 (1930); 2, 337 (1931)

47. M. Reiner, J. Rheol. 1, 250 (1930); 2 337 (1931)

48. B. Rabinowitsch, Z. physik. Chem. A145, 1 (1929)

49. R. K. Schofield and G. W. Scott Blair, J. Phys. Chem. 34 248 (1930); 35, 1212 (1931)

50. M. Mooney, J. Rheol. 2, 210 (1931)